VOL. 37, Nº 1 JUNIO 2014 ISSN 0717-2915

Revista Journal SELPER

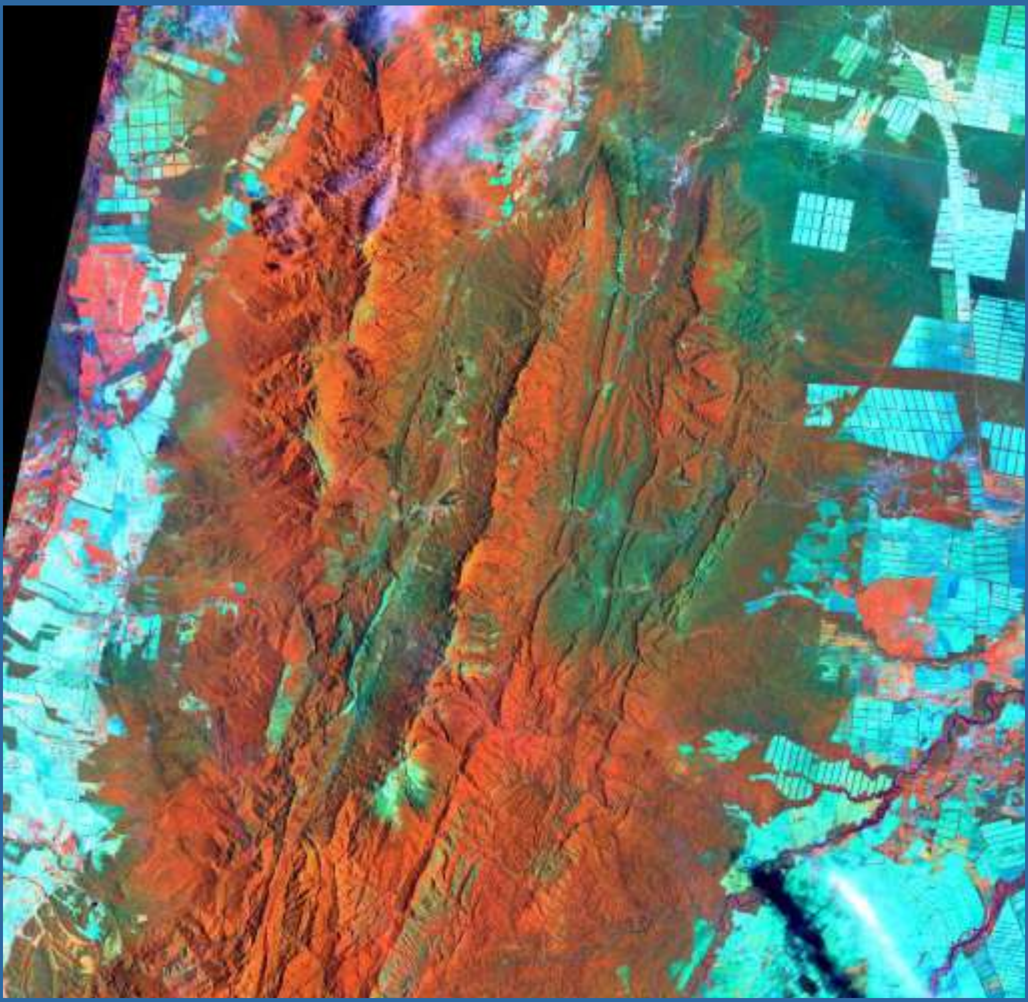

Yungas
Imagen de satélite LandSat 8 OLI

REVISTA JOURNAL

SOCIEDAD LATINOAMERICANA DE PERCEPCION REMOTA Y SISTEMAS DE INFORMACION ESPACIAL• SOCIEDADE LATINO-AMERICANA EM SENSORIAMENTO REMOTO E SISTEMAS DE INFORMAÇAO ESPACIAL• LATINAMERICAN SOCIETY ON REMOTE SENSING AND SPACE INFORMATION SYSTEM

SELPER

VOL. 37 Nº 1 JUNIO 2014 ISSN 0717-2915

FOTO PORTADA

Yungas

Imagen de satélite Landsat 8 OLI, resolución espacial 30 metros, en composición 5,6,4 / RGB, de la provincia de Salta y Jujuy tomada el día 4 de enero de 2014. Los sectores que se destacan son: Palma Sola, Reserva Natural Pizarro, Santa Clara y parte de la selva de yungas.

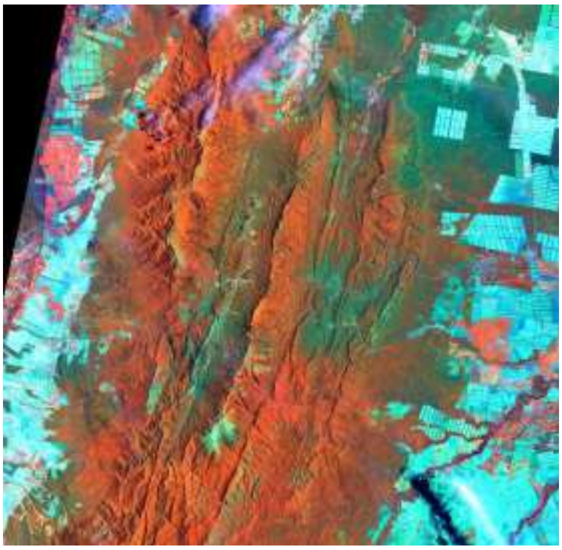

DIRECTORIO SELPER, SEDE Francia 2012 - 2014

Institut de recherche pour le développement Le Sextant
44, bd de Dunkerque, CS 90009 - 13572 Marseille cedex 02
Tél. 33 (0)4 91 99 92 00 - Fax 33 (0)4 91 99 92 22
selper.internacional@gmail.com

PRESIDENTE
Laurent Durieux
Francia

VICE–PRESIDENTE
Marie José Lefevre Fonallosa
Francia

VICE-PRESIDENTE
Silvia Casas
México

VICE-PRESIDENTE
Luz Angela Rocha
Colombia

RESPONSABLE DE DIVULGACIÓN ELECTRÓNICA
Fabián Lozano García
Mexico

COMITÉ DE RELACIONES INTERNACIONALES
Luz Angela Salamanca (Colombia)
Presidente interina
Laurent Durieux – Francia
Pedro Luis García Pérez - Cuba
Pedro Martínez Fernández - Cuba
Olga Piedad Rudas - Colombia
Anyul del Pilar Mora - Colombia
Luis Geraldo Ferreira - Brasil
Washintong Franca Rocha - Brasil
Victor Barrena - Perú

COMITÉ EDITORIAL
María Cristina Serafini (Argentina)
Presidente
Miriam Esther Antes – Argentina
Fabián Lozano – México
Leila María Fonseca – Brasil
Jorge Martín Chiroles - Cuba
Francisca Celia González - Argentina
Freddy Flores – Venezuela

COMITÉ DE EDUCACIÓN
Maria Antonia García Cisnero (Cuba)
Presidente
Luz Angela Rocha Salamanca - Colombia
Laura Delgado - Venezuela
Ethel Rubín de Celís Llanos - Perú
Josselisa Ma. Chávez - Brasil

COMITÉ DE PROYECTOS INTERNACIONALES
Paulo Roberto Martini (Brasil)
Presidente
Christopher Charron – Francia
Alfredo Cuello – Argentina
Miembro del ISPRS

CAPÍTULOS CONSTITUIDOS

ARGENTINA
Miriam Esther Antes
Universidad Nacional de Luján (PRODITEL)
Fuerza Aérea Argentina (CSR)
Cruce Rutas 5 y Ex. 7 (6700)
Luján, Buenos Aires, Argentina
Tel: 54 - 2323- 420380 - int. 248
Fax: 54 - 2323- 425795
E-mail: selperargentina@gmail.com

BOLIVIA
José Luis Liseca
Carrera de Topografía y Geodesia
Facultad Técnica
Universidad Mayor de San Andrés
Av. Arce 2299 1º Piso
La Paz, Bolivia
Tel.: 591-2-2441401
E-mail: jlisec@hotmail.com

BRASIL
Laércio Massuru Namikawa
INPE
Av. Dos Astronautas 1758, Sao José dos Campos
San Pablo, Brasil
Tel: 55 - 12-39456000
E-mail: laercio@dpi.inpe.br

CHILE
Héctor Gutiérrez Méndez
Centro Nacional de Información Aeroespacial
Antonio Varas 175
Oficina 310. Providencia
Tel: 562 -2362714
E-mail: hector.gutierrez@cenia.cl

COLOMBIA
Luz Angela Rocha Salamanca
Carrera 30 No. 48-51 Edificio IGAC-CIAF Of. 212
Bogotá D.C., Colombia
Tel: 57-1-369-4096
Fax: 57-1-369-4096
E-mail: lrochas@selper.org

CUBA
Pedro Luis García Pérez
Sede UNAICC, Humboldt No. 104,
Esquina a Infanta, Vedado, La Habana, Cuba
Telf.: (5 37) 8363447
E-mail: lgarcia@ch.unaicc.cu

ECUADOR
Cor. Ricardo Urbina
CLIRSEN
Edif. Instituto Geográfico Militar, Piso 4
Seniergues s/n y Paz y Miño
Apartado Postal 17-08-8216

GUATEMALA
Carlos Alberto Duarte
Ingeniería Virtual
Ruta 4, 6-49 Zona 4, Oficina 14
Ciudad de Guatemala (01004), Guatemala
Tel: 502 - 334-1039/4038
Fax: 502 - 331-9390
E-mail: chduarte@hotmail.com

GUYANA FRANCESA
Laurent Polidoril
Directeur de Recherche IRD / US ESPACE 140
Institut de Recherche pour le Développement (ex-ORSTOM)
Route de Montabo - BP 165 - 97323 Cayenne cedex
Tel. (+594) 594 29 92 81
Fax (+594) 594 31 98 55
E-mail:polidori@cayenne.ird.fr

MÉXICO
Jean Francois Mass
UNAM Campus Morelia
Morelia, Michoacan, México
E-mail: jfmas@ciga.unam.mx

FRANCIA
Marie José Lefevre Fonollosa
CNES
18 avenue Edouard Belin, 31401 Toulouse Cedex 9
Tél : 3305 61 27 4283
Fax : 3305 61274842
E-mail: marie-jose.lefevre @cnes.fr

URUGUAY
Antonio Alarcón
Servicio de Sensores Remotos Aeroespaciales Fuerza Aérea Uruguaya
Ruta 101 s/n Km. 19500
Carrasco, Canelones, Uruguay
Tel.: 598 -2 601 4083
Fax: 598 -2 601 4090
E-mail: aalarconv@hiotmail.com

VENEZUELA
Ramiro Salcedo
Centro de Procesamiento Digital del Instituto de Ingenieria en Caracas
Apdo. Postal 40200 / Caracas, Venezuela
Tel/fax: 58 - 212 - 903 -4682
E-mail: ramiros@fii.org

PERÚ
Victor Barrena Arroyo
Universidad Nacional Agraria La Molina
Av. La Universidad s/n
La Molina, Lima, Perú
Tel / Fax: 51-1-349-5647 anexo 232/349-2041

CAPÍTULOS EN FORMACIÓN

PARAGUAY
Sergio M. Burgos Sosa
IPPA
Dr. César Sánchez 431
San Lorenzo, Paraguay
Tel/Fax: 595- 21-574909
Email: smburgos@highway.com.py

CAPÍTULOS ESPECIALES

ALEMANIA
Klaus Reiniger
DLR
D-8031 Oberpfaffenohfen
Alemania
Tel: 49- 8153- 281.189
Fax: 49- 8153- 281.443

CANADÁ
Fritz P. Dubois
25 Nidland
Crs Nepean Ontario Kh2-8n2
Ontario, Canadá
Tel: 613- 596-4164
Fax: 613- 723-9626

ESPAÑA
José L. Labrandero
Consejo Superior de Investigaciones Científicas (CSIC)
Pinar 25- Madrid 28006, España
Tel: 34- 411.10.98
Fax: 34- 562.55.67

HOLANDA
Carlos Valenzuela
ITC
350 Boulevard 1945, P.O.X. 6. 7500 AA
Enschede, Holanda
Tel.: 31 53 874-444
Fax: 31 53 874-400

ITALIA
Francesco Sarti
ESA/ESRIN
Via Galileo Galilei, s/n
I-00044 Frascati, Italia
Tel: 39 - 694180409
Fax: 39 - 694180602
E-mail: Francesco.Sarti@esa.int

Maurizio Fea
via Alessandro Poerio, 49
00152 Roma
tel/fax: +39065880581
móvil: +393281771383
E-mail: maufea@gmail.com

USA
Patricia M. Ravelo
SPOT
Estados Unidos
Tel: 1-800-ask-spot ext. 137
Fax: 703-648.1813
E-mail: ravelo@spot.com

COMITÉ EDITORIAL

COMITÉ DE EVALUADORES

- **Análisis de parámetros morfométricos y su relación con condiciones de vulnerabilidad en la ecorregión de las Yungas, Argentina**
  Maria C. Serafini
  Maurizio Fea
  Leonardo Di Franco
  Alfredo Cuello
  Miriam Antes
  Solange Villanueva
  Walter Sione 5

- **Identificação prévia de talhões de soja no Mato Grosso a partir de imagens MODIS – avaliação do mapeamento**
  Isaque Daniel Rocha Eberhardt
  Rodrigo Rizzi
  Joel Risso 14

- **Mud banks, sand flux and beach morphodynamics in French Guiana: A remote sensing approach**
  Edward Anthony
  Antoine Gardel
  Franck Dolique
  Andy Chatelet
  Christina Péron
  Benjamin Kulling
  Guillaume Brunier 21

- **Ocean color remote sensing in coastal waters of French Guiana: application of the ANR GlobCoast project**
  V. Vantrepotte
  H. Loisel
  X. Mériaux
  D. Dessailly
  A. Gardel
  E. Gensac 28

Editado por: SELPER Internacional
Universidad Nacional de Luján
Rutas 5 y ex 7, (6700) Luján - Bs. As. ARGENTINA

EJEMPLAR DE DISTRIBUCIÓN GRATUITA PROHIBIDA SU VENTA

PLAN EDITORIAL SELPER 2012 - 2014

PLAN EDITORIAL SELPER

A partir de las decisiones adoptadas en el marco del XIII Simposio Latinoamericano de Percepción Remota y Sistemas de Información Espacial, llevado a cabo en La Habana, Cuba, en setiembre de 2008, la edición de la Revista SELPER está disponible en la página de nuestra Sociedad: http://www.selper.info.

En esta oportunidad hacemos llegar la publicación del volumen 37 Número 1., donde se incluyen trabajos que han sido presentados en el XIV Simposio Latinoamericano de Percepción Remota y Sistemas de Información Espacial (SELPER), desarrollado en Cayena, Guyana Francesa, en noviembre de 2012.

NORMAS PARA LOS AUTORES

Los artículos recibidos serán enviados a tres (3) expertos en la temática para su revisión. Los trabajos aprobados serán publicados en estricto orden, de acuerdo a las fechas de llegada de las contribuciones.

Los idiomas oficiales SELPER son: Español, Portugués e Inglés.

Los trabajos deberán estructurarse contemplando las siguientes secciones:

a) Título del trabajo. Nombre de los autores y direcciones completas

b) Resumen (no más de 150 palabras) indicando al final las palabras claves. Deberá incluirse en Español o Portugués, además de Inglés

c) Introducción

d) Objetivos

e) Metodología empleada y materiales

f) Resultados obtenidos

g) Conclusiones

h) Bibliografía: sólo se incluirá la citada en el texto. Se indicarán los autores, por orden alfabético, año, título, revista o medio donde fue publicado, incluyendo volumen y páginas, cuando corresponda.

Los títulos y subtítulos de cada sección deberán estar claramente indicados (ya sea con numeración o tamaño de letras). Las tablas, fotos y figuras deberán ser suficientemente nítidas, llevar un título y estar numeradas en forma consecutiva.

Se deberá enviar una copia del trabajo en formato Word y una copia papel. La extensión total del trabajo no deberá superar las 12 páginas, (DIN-A4).

Los trabajos se enviarán a: editorial@selper.org

Análisis de parámetros morfométricos y su relación con condiciones de vulnerabilidad en la ecorregión de las Yungas, Argentina

Maria C. Serafini 1; Maurizio Fea 2; Leonardo Di Franco 1; Alfredo Cuello 1-3; Miriam Antes 1-3; Solange Villanueva 1 y Walter Sione 1-4

1 PRODITEL- Dpto. de Ciencias Básicas - UNLu
2 Asociación Geofísica Italiana - AGI
3 C.S.R - Fuerza Aérea Argentina
4 CEREGEO – UADER - CEREGEO
proditel@unlu.edu.ar

RESUMEN

A principios del siglo XX, el sector continental argentino (2.791.810 km^2) se encontraba cubierto por, aproximadamente, 100 millones de hectáreas de bosques nativos, superficie que se redujo a 33 millones a finales del mismo; incrementándose en forma notoria la tasa anual de deforestación en los últimos 30 años. Parte de esa superficie forestal se desarrolla en las provincias de Salta y Jujuy, con alrededor de 5 millones de hectáreas que representan ecosistemas ambientalmente críticos para el mantenimiento de la biodiversidad regional. Los datos obtenidos a partir de los sensores remotos resultan un aporte significativo para la evaluación de los cambios producidos en estos ambientes. El presente trabajo se enmarca en el Proyecto denominado “Evaluación de cambios en áreas de monte nativo y su relación con situaciones de vulnerabilidad ambiental en la ecorregión de Selvas subtropicales andinas (Yungas) mediante la fusión de datos Radar – Ópticos” y tiene como principal objetivo generar insumos temáticos que serán utilizados en la elaboración de indicadores ambientales relacionados con la vulnerabilidad ambiental en esta ecorregión. La zona seleccionada corresponde al departamento Ledesma de la provincia de Jujuy, una de las dos Áreas pilotos definidas para llevar a cabo este estudio. Mediante imágenes de la Shuttle Radar Topography Mission (SRTM), disponibles gratuitamente en la web, fueron definidos parámetros geomorfológicos que permitieron establecer el comportamiento de determinadas variables. Los resultados obtenidos corresponden a diferentes capas temáticas relacionadas con parámetros como: Sombreado analítico, pendiente, aspecto, zona de captación, Índice de humedad, Factor LS, limitación de subcuencas y red hídrica secundaria, los que a partir de su integración en un Sistema de Información Geográfica permitirán contribuir en la elaboración de indicadores relacionados con la vulnerabilidad ambiental en la zona bajo estudio.

Palabras clave: Yungas - parámetros geomorfológicos – teledetección – SIG - vulnerabilidad

ABSTRACT

In the early twentieth century, the continental sector of Argentina (2,791,810 km^2) was covered by about 100 million hectares of native forest area. This area was reduced to 33 million by the end of the century. Over the last 30 years the anual deforestation has noticeably increased. Part of the forest area is in Salta and Jujuy provinces, with about 5 million hectares representing critical environmental ecosystems for the regional biodiversity maintenance. The remote sensor data are a significant contribution for environment change evaluation. This work belongs to the Project: "Evaluation of changes in native forest areas and their relation with environmental vulnerabilities in subtropical Andean Forest ecoregion (Yungas) using radar – optical data fusion". The aim of this study was to generate thematic inputs in order to use them for the development of environmental indicators related to the environmental vulnerability in this ecoregion. The selected area belongs to Ledesma department (Jujuy province) and is one of the two selected study sites to carry out this work. Geomorphological parameters were defined using Shuttle Radar Topography Mission (SRTM) images, which are freely available in the web. These parameters were useful to settle down certain variable behaviour. These results correspond to different thematic layers related to parameters such as analytical shading, slope, aspect, catchment area, moisture index, LS factor, watersheds delimitation and secondary hydric network. The integration of these parameters into a GIS system will contribute to the development of indicators related to environmental vulnerability in the under study area.

Keywords: Yungas - geomorphological parameters - Remote sensing - GIS-vulnerability

INTRODUCCIÓN

Entre los problemas ambientales que causan mayor preocupación a nivel mundial merecen citarse los que se relacionan con la degradación de las tierras. En Argentina son diversas las actividades que se desarrollan en este sentido y colocan en situación de severo riesgo a ambientes naturales, generando conflictos socio-ambientales de diversa magnitud; entre otras, la minería a cielo abierto (Donadio, et al. 2009), la introducción de especies exóticas y la incorporación de extensas áreas de monte nativo a la actividad agrícola (Paruelo, et al. 2005).

En los últimos años, la sobreexplotación de los recursos forestales muestra un acelerado incremento; esta situación se presenta en la mayor parte de los montes nativos de nuestro país donde se vienen implementando acciones tendientes a aumentar la productividad, las que han generado situaciones problemáticas de transformación de sus espacios, así como de un aprovechamiento irracional de los recursos naturales. En el caso particular de la Selva Tucumano-Oranense, también denominada Yungas, el impacto antrópico ha favorecido la fragmentación del paisaje a partir del avance de la frontera agropecuaria, afectando en forma negativa la biodiversidad de dicho ecosistema, dando origen a condiciones de vulnerabilidad ambiental.

La vulnerabilidad, en términos generales, es la relación entre una condición, susceptible de recibir daño, en referencia a otra, condición no dañada, donde se manifiesta el orden, el peligro y el riesgo (Macias, 1999). La vulnerabilidad ambiental es un concepto que se relaciona con la susceptibilidad o predisposición intrínseca del medio y los recursos naturales a sufrir un daño o una pérdida, siendo estos elementos físicos o biológicos (Gaspari, et al; 2011).

El análisis conjunto de factores que permiten definir situaciones de vulnerabilidad ambiental se ha facilitado con la introducción de los Sistemas de Información Geográfica (SIG), herramienta ideal para el análisis de parámetros con un alto grado de variabilidad espacial.

Desde la puesta en órbita de los primeros satélites, hasta el presente, el desarrollo de las tecnologías espaciales ha evolucionado de manera continua; las imágenes o productos elaborados a partir de datos aportados por los satélites de observación terrestre se encuentran disponibles en diferentes servidores y suponen una fuente de datos para los SIG (Buzai, G., 2000).

Su aplicación a los recursos hídricos y en particular al manejo de cuencas, resulta una herramienta indispensable para conocer el ambiente y de esta manera hacer un uso sustentable del mismo. Un ejemplo de ello lo configuran los parámetros geomorfológicos derivados de imágenes topográficas que permiten establecer el comportamiento de determinadas variables y ser incluidos en modelos más complejos como la Ecuación Universal de Pérdida de Suelos (USLE), entre otros (Di Franco, et al; 2012).

Las imágenes de la Shuttle Radar Topography Mission (SRTM), disponibles gratuitamente en la web, favorecen la extracción de estos parámetros brindando información topográfica del área (NASA, 2005).

El presente trabajo se enmarca en el Proyecto denominado “Evaluación de cambios en áreas de monte nativo y su relación con situaciones de vulnerabilidad ambiental en la ecorregión de Selvas subtropicales andinas (Yungas) mediante la fusión de datos Radar – Ópticos” y tiene como principal objetivo generar insumos temáticos que serán utilizados en la elaboración de indicadores ambientales relacionados con la vulnerabilidad ambiental en esta ecorregión.

MATERIALES Y MÉTODOS

Área de estudio

La zona seleccionada para llevar a cabo este estudio comprende el departamento Ledesma, uno de los 16 departamentos de la provincia de Jujuy; corresponde a una de las dos Áreas Pilotos definidas para llevar a cabo el Proyecto marco. Este departamento se encuentra situado al este de la provincia de Jujuy, sus coordenadas geográficas lo ubican entre los 63º30' y los 65º20' de longitud oeste y los 23º45' y 24º00' de latitud sur. Posee una superficie de 3.249 km^2, limita al norte con la provincia de Salta, los departamentos Tilcara y Valle Grande, al este con el departamento Santa Bárbara, al sur con el departamento San Pedro y al oeste con los departamentos Doctor Manuel Belgrano y Tumbaya. Pertenece a la ecorregión de las Yungas, también llamadas Selvas Subtropicales de Montaña o Selva Tucumano-oranense; está definida por una franja de aproximadamente 700 km de longitud norte-sur y 50 km de ancho, que se extiende a lo largo de las laderas orientales de las montañas del norte del país, en las provincias de Salta, Jujuy, Tucumán y Catamarca (Figura 1). Abarcan las laderas y valles, con alturas que van de 400 msnm, al este hasta los 3.000 msnm, al oeste. Aunque sólo representan el 2% del territorio nacional, junto con la Selva Misionera constituyen los ambientes de mayor riqueza de especies y recursos naturales de nuestro país. En conjunto, albergan alrededor del 50% de la biodiversidad de Argentina. Las serranías que la circundan son: Calilegua y Santa Bárbara. El clima, subtropical con estación seca, está caracterizado por un régimen térmico altamente influenciado por el relieve, afectándolo fundamentalmente, la latitud y altitud; la temperatura media anual es de 21,5º C, siendo enero el mes más cálido, con temperatura máxima de 28,2 ºC y julio el mes más frío con 13,5 ºC.

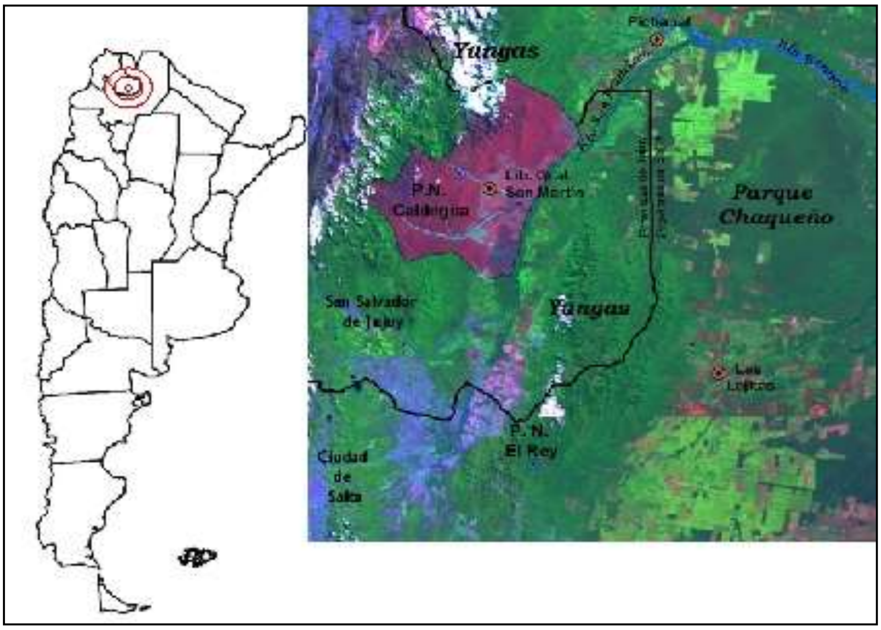

Figura 1. Ubicación del área de estudio

Materiales y Métodos

Para la realización de este trabajo se utilizaron dos imágenes correspondientes a la Shuttle Radar Topography Mission (SRTM), Path and Row 231/076 y 231/077 de fecha febrero de 2000. Estas imágenes son generadas a partir de datos radar en banda C con una longitud de onda de 5,6 cm. La descarga de los datos se realizó a partir de la web de la Universidad de Maryland; el tipo de SRTM correspondió al Unfilledfinished_B, que presentaba algunos valores anómalos que fueron corregidos mediante el proceso de interpolación (Sanders, 2007; Verdin, et al, 2007). El SRTM tiene una resolución espacial de 90 metros, radiométrica de 16 bit y formato geotiff (Farr, 2007).

Para poder realizar la delimitación de la cuenca del río San Francisco, principal curso del departamento de Ledesma, que recibe varios afluentes por su margen izquierda, entre otros el Negro, el Ledesma, el San Lorenzo y el de Las Piedras y por su margen derecha, los ríos del Medio, de las Conchas y Santa Rita, fue necesario generar un mosaico a partir de las dos escenas adquiridas ya que el área comprendida por la misma excedía las imágenes individuales; este mosaico fue generado mediante el empleo de la herramienta Mosaic Tools, del ERDAS.

Una vez obtenido el mosaico satelital se procedió a la delimitación de la cuenca mediante el empleo de la herramienta de Hidrología con el software ARCGIS 10.1. El procedimiento para la delimitación incluyó la corrección de los valores anómalos presentes en el SRTM, identificados con el valor -32768. Este procedimiento se realizó con la herramienta Fill Skins. Además de corregir estos valores permite completar aquellos lugares denominados sumideros en donde el escurrimiento presenta incongruencias. En la Figura 2 se puede observar el mosaico generado, con valores anómalos (a) y el mosaico obtenido luego de la interpolación y corrección a través de la herramienta Fill skins (b).

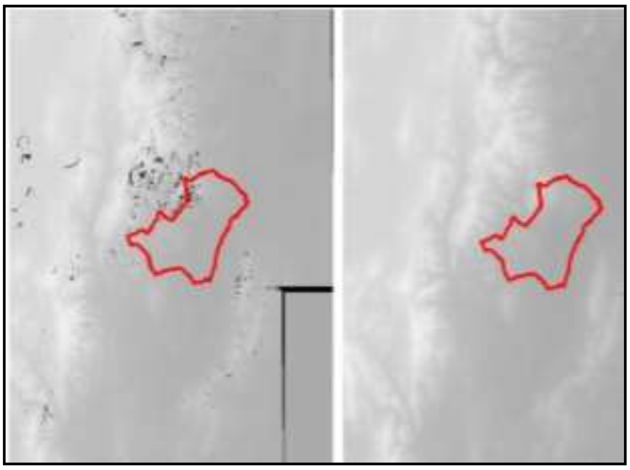

(a) (b)

Figura 2. Mosaico SRTM con huecos, presencia de valores anómalos (a) y corregido (b)

El paso siguiente consistió en la obtención de la capa temática denominada Flow direction que crea un raster de dirección de flujo desde cada celda hasta su vecina. En esta nueva capa raster el valor asignado a la celda puede contener ocho valores que corresponden a la dirección de flujo. La capa Flow accumulation, que crea un raster de flujo acumulado a partir de la cantidad de celdas que aportan a ella, en conjunto con la capa Flow direction, configuran los principales insumos para calcular los parámetros.
Para definir los límites topográficos de la cuenca bajo estudio se utilizó la herramienta Cuenca hidrográfica, ésta genera una capa raster que posteriormente se convierte a formato vectorial. Mediante la utilización de estas capas raster se extrajo la red hídrica principal y secundaria. Una vez identificada la cuenca principal se procedió a la delimitación de las diferentes subcuencas utilizando como punto de afogue la unión de los diferentes tributarios con el cauce principal. En la Figura 3 se puede observar la red hídrica principal y secundaria (a) y la delimitación de las diferentes subcuencas dentro del departamento de Ledesma (b).

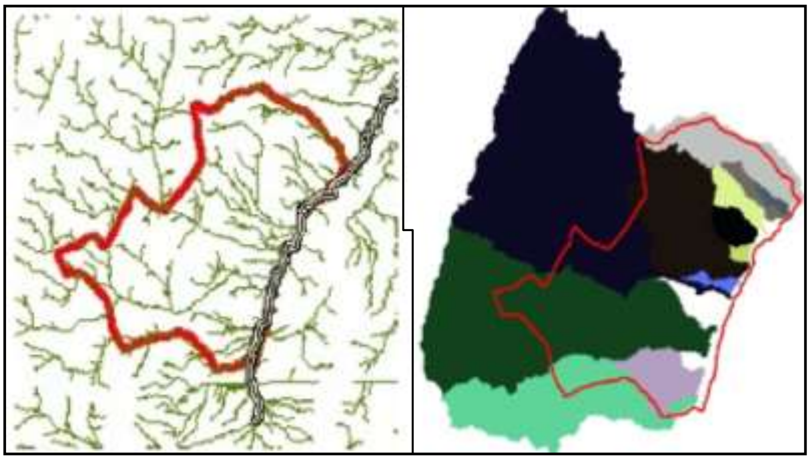

(a) (b)

Figura 3. Red hídrica principal y secundaria (a) y delimitación de las diferentes subcuencas dentro del departamento de Ledesma (b)

Una vez completados los pasos metodológicos tendientes a delimitar las cuencas y subcuencas del área de estudio, se procedió con la segunda etapa del trabajo que consistió en seleccionar los parámetros morfológicos para describirla, utilizando los criterios de la hidrología superficial. Esta etapa se realizó con el programa SAGA (System for Automated Geoscientific Analyses) un software enmarcado en Free Open Source Software (FOSS), desarrollado por el Departamento de Geografía Física de Gottingen, Alemania. La herramienta seleccionada fue Basics Terrain Analysis que permitió escoger siete entre los once parámetros morfométricos disponibles. Los parámetros seleccionados fueron:

- Factor LS: factor de inclinación de la pendiente (S) y de su longitud (L), muy utilizado en la Ecuación Universal de Perdida de Suelo (USLE) y en la Ecuación Universal de Perdida de Suelo Revisada (RUSLE). Es un parámetro adecuado para evaluar el riesgo de erosión a escala de cuenca.
- Índice de humedad topográfica: se utiliza para describir patrones espaciales de humedad en una región. Se calcula a partir de la pendiente, siendo húmedas aquellas zonas donde las pendientes son bajas y sus áreas de contribución grandes, y las secas corresponden a mayor pendiente y menor área de contribución.
- Índice de convergencia: Es un indicador de la configuración o forma del terreno siendo las áreas cóncavas las que concentran el drenaje superficial mientras que las convexas diluyen el drenaje hacia celdas vecinas.
- Zona de captación: es el área geográfica donde el agua superficial drena hacia un punto determinado.
- Sombreado analítico: es una simulación de sombreado basada en valores de iluminación solar sobre la superficie terrestre con propósitos cartográficos. El efecto visual esta dado por la diferenciación en los tonos de la imagen resultado.
- Pendiente: definida como el ángulo existente entre el vector normal a la superficie en ese punto y la vertical.
- Aspecto: se puede definir como la dirección de la pendiente y se mide en grados (0° a 360°) en tanto que las zonas planas poseen un valor de -1.

En la Figura 4 se plantea el esquema metodológico que incluye los principales pasos realizados para la obtención de los parámetros definidos para este estudio, los que posteriormente serán integrados en un SIG desarrollado *ad hoc*.

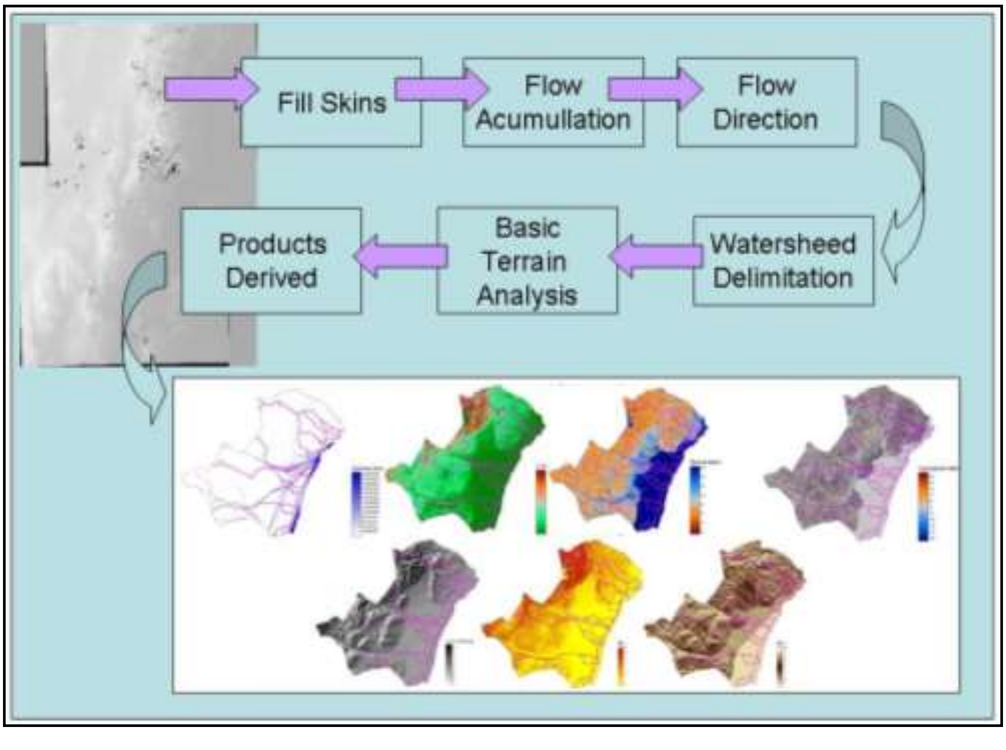

Figura 4. Esquema metodológico

RESULTADOS

La metodología aplicada para evaluar los parámetros morfométricos en el área bajo estudio proporcionó como resultados la siguiente caracterización:

Factor LS: Este factor topográfico muestra las zonas con mayor potencial de erosión hídrica, que en la imagen aparecen en colores marrones oscuros mientras que las zonas donde se realiza la deposición del material extraído corresponden a colores verdes oscuros. En función de este parámetro se pueden determinar, en las diferentes subcuencas, las áreas con mayor riesgo de deslizamiento. En estas zonas resulta elemental conservar la cobertura boscosa para minimizar las consecuencias de este tipo de fenómenos (Figura 5).

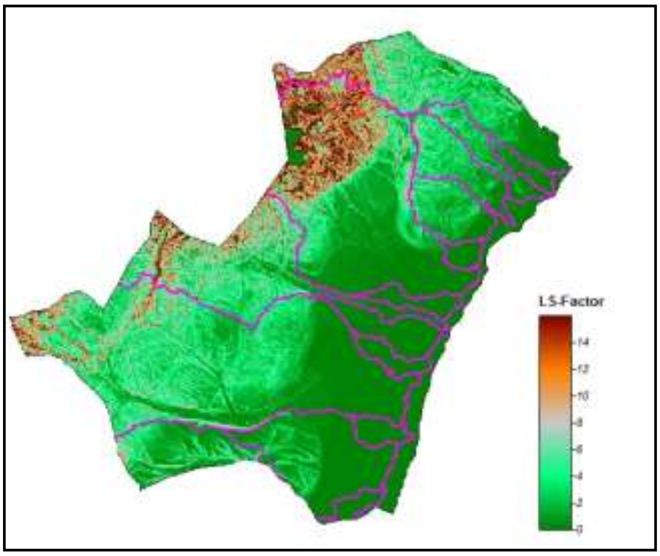

Figura 5. Niveles del Factor topográfico LS

Índice de humedad topográfica (TWI): Este índice resulta útil para cuantificar el control de la topografía en los procesos hidrológicos e indicar la espacialidad de la humedad del suelo y la saturación de la superficie. En el oeste del departamento, lugar donde las pendientes son máximas, indicadas en colores ocres, el índice presenta los valores de menor potencial de retención de humedad de suelo, mientras que aquellas zonas correspondientes a las áreas planas, indicadas en colores azules, presentan mayores potenciales de retención y saturación (Figura 6).

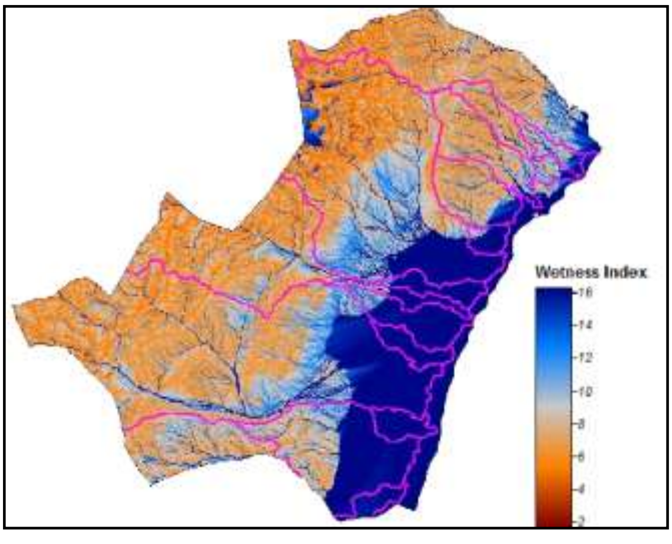

Figura 6. Niveles de Índice de humedad topográfica (TWI)

Índice de convergencia: Este factor se calculó teniendo en cuenta las celdas adyacentes, su aspecto y su relación con la celda central. Determinó como decrece o crece la celda circundante en relación a la central. La imagen resultante del análisis de este factor permite establecer, para cada subcuenca, las áreas neutras en relación al drenaje superficial (tonos grises) (Figura 7).

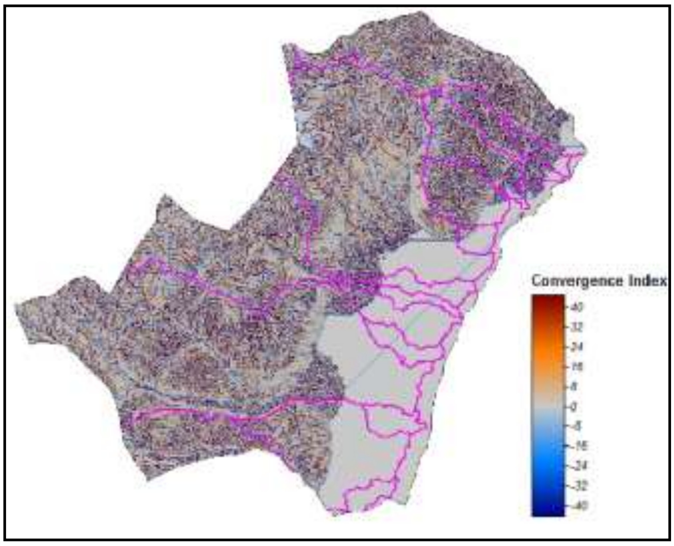

Figura 7. Niveles de Índice de Convergencia

Zona de captación: En este factor se determina el tamaño del área de aporte en cada subcuenca. Las zonas de color blanco representan el área de captación mientras que las de color azul representan la red hídrica por donde el agua escurre transportando sedimentos (Figura 8).

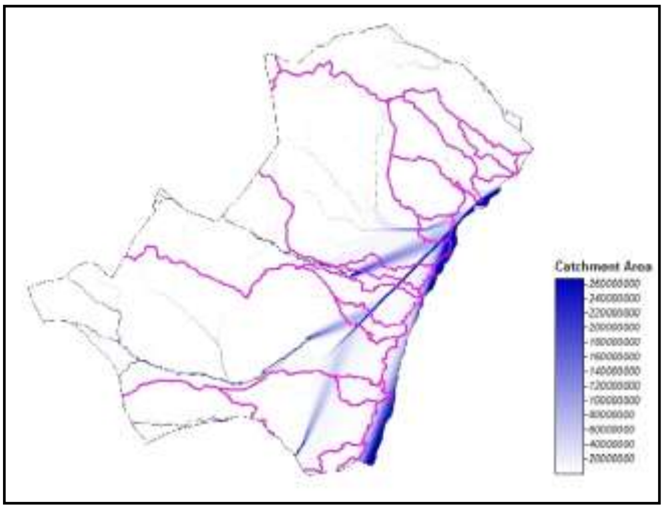

Figura 8. Zona de captación y red hídrica con transporte de sedimentos

Sombreado analítico: este tipo de raster permite crear mapas que favorecen la interpretación al facilitar la comprensión del relieve, ya que tienen en cuenta como la luz del sol iluminaría la superficie en un punto dado para una posición particular. En este producto se observa que aquellas laderas que resultaron con menor iluminación aparecen en tonos oscuros mientras que las mayores iluminaciones se observan en tonos claros (Figura 9).

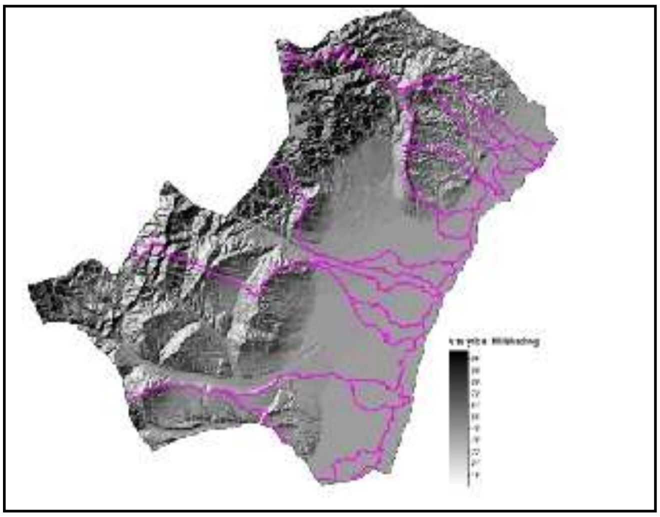

Figura 9. Sombreado analítico

Pendiente: muestra las áreas de fuerte pendientes en tonos rojizos que indican, en este caso, aquellas zonas críticas con respecto a la perdida de suelo por erosión hídrica. Como medida de conservación se debe proteger la cubierta boscosa dado que el riesgo de erosión es elevado. Mientras que las zonas de tonos amarillos representan las áreas con menor pendiente y por lo tanto menor factor de erosión (Figura 10).

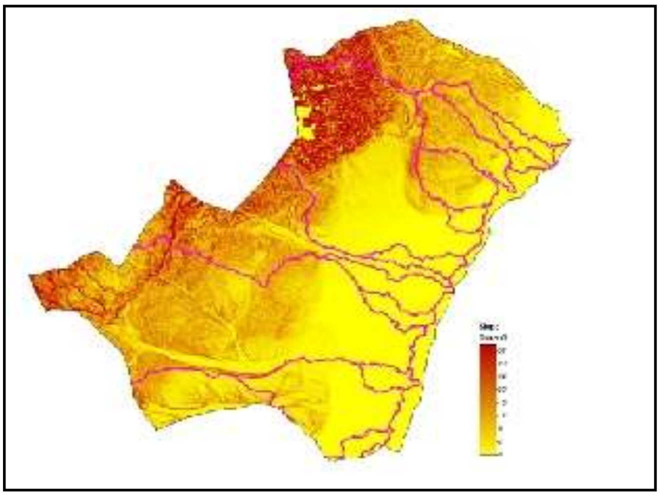

Figura 10. Pendiente

Aspecto: La dirección de la pendiente muestra la forma de exposición de la superficie. En general las laderas de exposición norte (tonos claros) presentan suelos con menor contenido de humedad que las laderas de exposición sur (tonos oscuros) y por lo tanto menor cobertura vegetal y más bajo contenido de materia orgánica representando suelos más erodables (Figura 11).

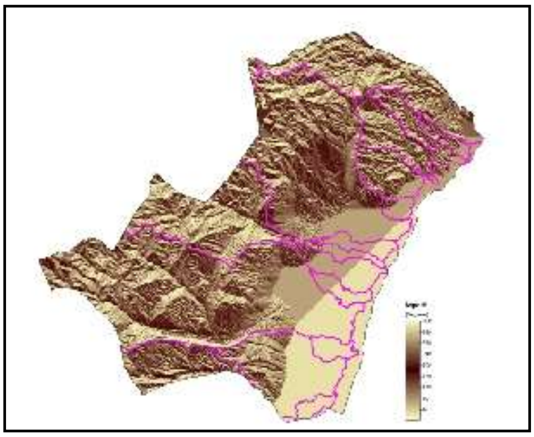

Figura 11. Aspecto

CONCLUSIONES

Los parámetros de sombreado analítico, pendiente y aspecto describen características del relieve de la cuenca que permiten una mejor visualización de la misma; tanto la pendiente como el aspecto presentan relación con las características morfométricas lineales y el relieve de las diferentes subcuencas**.**

En base al análisis de los diferentes parámetros seleccionados se pudo establecer el comportamiento hidrológico de la cuenca. El mismo se encuentra íntimamente relacionado con la topografía y con las características fisiográficas.

Los resultados obtenidos en el presente estudio aportan información temática en formato raster; la integración de estas capas en un SIG permitirán realizar un análisis espacial más complejo que conducirá a una adecuada evaluación y diagnóstico de las condiciones que afectan la vulnerabilidad ambiental, estableciendo mejores estrategias de gestión y planificación sustentables en ambientes amenazados.

Una etapa posterior debería incluir información de uso y cobertura de la tierra basándose en datos satelitales.

BIBLIOGRAFÍA

Buzai, G., (2000): La exploración geodigital. Lugar Editorial S.A., Buenos Aires, Argentina

Di Franco, L.; Cuello, A. y Serafini, M. C. (2012): "Parametrización de la cuenca hidrográfica del río Luján, Argentina, basada en Geomática", Proceedings XV Simposio SELPER Internacional; Cayena, Guyana Francesa

Donadío, E. (2009): "Ecólogos y mega-minería, reflexiones sobre por qué y cómo involucrarse en el conflicto minero-ambiental"; Ecología Austral, 19(3), págs. 247-254

Farr, T. G. (2007): "The Shuttle Radar Topography Mission"; Geophys, 45, RG2004, DOI:10.1029/2005 RG000183, págs. 21- 22.

Gaspari, F. J.; Rodriguez Vagaría, A. M.; Delgado, M. I.; Senisterra, G.E y G.A. Denegri (2011): "Environmental vulnerability in rangeland watersheds, using a GIS Multequina, ISSN 0327-9375, 20, págs. 3-13

Macias, J. M. (1999): "Desastres y protección civil. Problemas sociales, políticos y organizacionales". Centro de Investigaciones y Estudios Sociales en Antropología Social". Dirección General de Protección Civil del Gobierno del Distrito Federal, México. pág. 101

NASA (2005): Shuttle Radar Topography Mission: Instruments. http://www2.jpl.nasa.gov/srtm/instr.htm (Version 06 August 2008)

Paruelo, J.M.; Guerschman, J. P. y S. Verón (2005): "Expansión agrícola y cambios en el uso del suelo"; Ciencia Hoy 15, págs. 14-23

Sanders, B. F. (2007): "Evaluation of on-line DEMs for flood inundation modeling"; Advances Water Res.; V. 30, págs. 1831 – 1843

Verdin, K.L.; Godt, J.W.; Funk, C.; Pedreros, D.; Worstell, B. y J. Verdin (2007): "Development of a global slope dataset for estimation of landslide occurrence resulting from earthquakes"; Colorado, U.S. Geological Survey, Open-File Report 2007-1188, pág. 25

AGRADECIMIENTOS

Los autores expresan su agradecimiento a la Comisión Nacional de Actividades Espaciales (CONAE) por el aporte recibido para el desarrollo del presente trabajo.

Identificação prévia de talhões de soja no Mato Grosso a partir de imagens MODIS – avaliação do mapeamento

Isaque Daniel Rocha Eberhardt 1; Rodrigo Rizzi 1 e Joel Risso 2

1 – Universidade Federal de Pelotas UFPel
Campus Universitário S/N. Caixa Postal 354, 96.001-970 - Capão do Leão - RS, Brasil
2 – Instituto Nacional de Pesquisas Espaciais – INPE
Av. dos Astronautas, 1758. Caixa Postal 515, 12.227-010 – São José dos Campos - SP, Brasil
isaquedanielre@yahoo.com.br

ABSTRACT

The CEI Preview Estimate (CEI-PE) is an alternative approach that uses images acquired prior to peak canopy development to antedate soybean detection up to 45 days comparing to the original CEI technique. Our goal in this paper is to assess three preview soybean mapping in municipal level by using CEI-PE over Mato Grosso State in crop year 2005/2006. To compose MaxEVI, the last image used by the original CEI in Mato Grosso State is a 16-day composited EVI MODIS image acquired from Day Of Year (DOY) 49 to 65 (MaxEVI-65). In the three CEI-PE we composed MaxEVI using images acquired up to DOY 49, 33, and 17, retrieving CEI-49, -33, and -17 mapping, respectively. Finally, we compared CEI-PE against original CEI map to look into mapping errors in 42 municipalities that comprised 92% of the State soybean acreage. Our results showed decreasing errors in soybean mapping from CEI-17 to -49 for all municipalities. Likewise, we identified 22, 7 and 3 municipalities with spatial accuracy over 90% in CEI-49, -33 and -17 mappings, respectively. Furthermore, omission errors were higher than commission ones in all CEI-PE as well as more intense in the southeastern portion of the State. We also noticed smaller errors over municipalities with large soybean area within the main producing regions for all CEI-PE mappings. Nevertheless, we observed large errors also in CEI-49, indicating that the composited MODIS image acquired from DOY 49 to 65 was crucial to map soybeans fields for those municipalities.

Keywords: Area estimation; vegetation index; spatial agreement; MODIS

1. INTRODUÇÃO

A agricultura é a base fundamental para a segurança alimentar das populações e uma das principais atividades econômicas da atualidade. A soja ocupa posição de destaque entre os cultivos mais importantes na agricultura mundial, com 102 milhões de hectares cultivados na safra 2011/2012 (USDA, 2012). Para a mesma safra o Brasil cultivou uma área superior a 25 milhões de hectares de soja (IBGE, 2012; USDA, 2012) e o estado o Mato Grosso (MT) apresentou 27% da área cultivada no país nessa safra (IBGE, 2012). Esta cultura gerou ao Brasil aproximadamente 75 milhões de toneladas de grãos na safra 2010/2011 (CONAB, 2012a; USDA, 2012). Deste total, parte foi destinada às exportações, gerando 24 bilhões de dólares em divisas para o país (CONAB, 2012b). Estes números tornam o Brasil segundo maior produtor e exportador mundial de soja (MDIC, 2010).

As formas de obtenção de informações sobre área cultivada e volume de produção de uma atividade agrícola são as mais diversas. Entretanto, as técnicas tradicionais utilizadas disponibilizam somente valores de área plantada, produtividade e produção, não indicando a localização espacial das áreas cultivadas. Logo, através destas técnicas não é possível conhecer a distribuição espacial dos cultivos em uma mesma safra, tão pouco no decorrer de várias safras. Quando buscamos valores de área cultivada, podemos utilizar os sensos agropecuários (Pino, 1999) ou levantamento sistemático para cultivos agrícolas realizado por amostragem, tal qual o Levantamento Sistemático de Produção Agrícola (LSPA; IBGE, 2002), realizado pelo IBGE (Pino, 2001). Entretanto, ambas as técnicas de estimativa contêm limitações quanto a agilidade de disponibilização de suas informações, capacidade de captar as pequenas variações entre safras, particularmente em áreas de fronteira agrícola, e dificuldade de adoção de ferramentas de controle dos erros em função dos custos relativamente altos para a sua realização.

Alternativamente a estes problemas, muitos trabalhos apontam a utilização de imagens padrão Landsat como opção para a geração de mapas de culturas e estimativas de área em escala regional (Rizzi & Rudorff, 2005; Rudorff et al., 2005). Estas imagens possibilitam o mapeamento das áreas por meio de fotointerpretação. Para tanto, são necessárias imagens adquiridas em momentos específicos para a cultura e a região em estudo. Entretanto, a presença de cobertura de nuvens neste tipo de imagem é o principal empecilho para a aplicação desta metodologia em grandes regiões, e quando o objeto de estudo são regiões tropicais, tal qual o MT, isso é ainda mais crítico (Asner, 2001).

Com o lançamento do Sensor orbital MODerate resolution Imaging Spectroradiometer (MODIS) e a disponibilização de imagens compostas ao longo de vários imageamentos efetuados pelo sensor, o problema de cobertura de nuvens foi minimizado. Isso tornou-se possível em função das características desse sensor, que realiza o imageamento completo do globo a cada dois dias. Assim, as composições são elaboradas com os pixels de melhor qualidade disponível no período (Leeuwen et. al, 1999; Huete et al., 1999; Didan & Huete, 2006). As imagens compostas podem ser utilizadas para reproduzir os diversos índices de vegetação, tal como o Enhanced Vegetation Index (EVI) (Huete et. al, 1997).

A partir das limitações impostas pelos métodos de mapeamento de áreas cultivadas anteriormente citados, Rizzi et al. (2009) desenvolveram o Crop Enhancement Index (CEI), para mapear e estimar as áreas de soja. De modo que sua configuração possibilita obter um mapa para a cultura da soja no MT a partir do início de março. Assim, a disponibilização desta informação pode não ser produzida em tempo suficiente para a antecipação de alguns movimentos de mercado pelos envolvidos na cadeia produtiva da soja. Além disso, projetos operacionais, que utilizam a metodologia CEI como base, tal como a Moratória da Soja (Rudorff et al., 2012) também demandam a informação antecipada sobre as áreas cultivadas com soja.

No intuito de antecipar o mapeamento e a estimativa de área cultivada com soja no estado do MT, Eberhardt et al. (2011) desenvolveram a metodologia Crop Enhancement Index-Preview Estimate (CEI-PE). Esta metodologia possibilita antecipar a identificação, o mapeamento e a estimativa de área com a cultura da soja em até um mês e meio em relação a metodologia CEI. Desta forma, disponibilizando sucessivamente três mapas de estimativa prévia, entre meados dos meses de janeiro e fevereiro. Entretanto, a exatidão espacial do mapeamento gerado através de CEI-PE foi avaliada somente em nível de estado, podendo assim, existirem erros concentrados em algumas regiões, não captados pela avaliação em nível estadual. Assim, o objetivo deste trabalho foi identificar o acerto espacial dos mapas de soja CEI-PE em nível municipal no MT na safra 2005/2006.

2. MATERIAL E MÉTODO

Foram definidos como objeto de estudo os principais municípios produtores de soja do MT que possuiram área cultivada com soja maior que 30 mil hectares na safra 2005/2006, de acordo com a metodologia CEI. Este critério restringiu a área de estudo a 42 municípios, distribuídos nas principais regiões produtoras de soja do MT na safra 2005/2006, os quais englobam 5,38 milhões de hectares de soja (92,4% do total cultivada no estado) (Figura1). As imagens utilizadas foram as de EVI (produto MOD13Q1) produzidas a partir de composições de 16 dias e com resolução espacial de 250 metros, adquiridas pelo sensor MODIS (Huete et al. 1999; Leeuwen et. al, 1999).

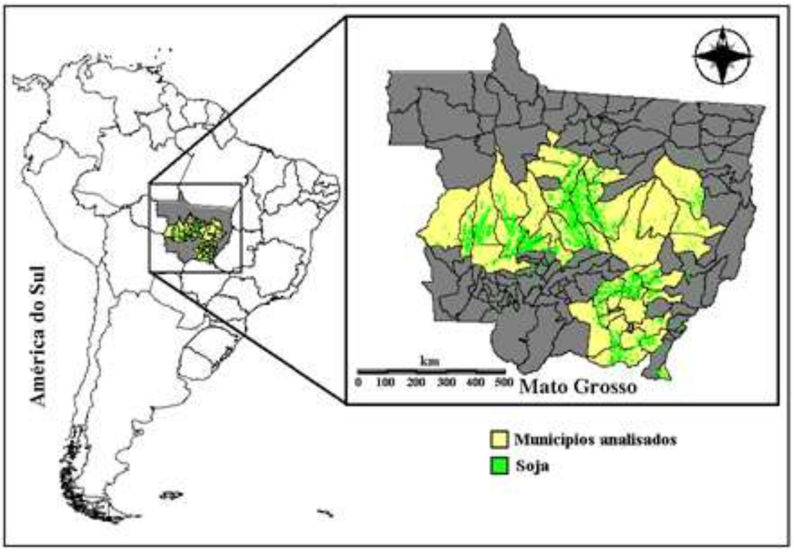

Fig. 1. Localização geográfica da área de estudo, no Estado do Mato Grosso.

A metodologia CEI usa imagens EVI adquiridas em dois períodos específicos da cultura da soja, chamados de Mínimo (MinEVI) e Máximo EVI (MaxEVI). No presente trabalho o MinEVI foi formado pelas imagens adquiridas entre os DA 161 e 224, extraindo o mínimo valor observado para cada pixel no período. Esta antecipação do período de composição do MinEVI teve por objetivo aproveitar o maior potencial de contraste do EVI entre as áreas de soja e demais classes de uso/cobertura do solo no período seco reduzindo a possibilidade de utilizar imagens contaminadas com nuvens e/ou sombra de nuvens que podem ocorrer a partir de setembro, quando inicia o período de chuvas no Mato Grosso (Risso et al., 2012). Semelhantemente, a partir das imagens adquiridas entre os DA 321 e 64, é obtido o MaxEVI. Assim, as imagens de Max e MinEVI são aplicadas na equação que retorna a máxima diferença registrada entre os períodos, nesta equação se utiliza ainda o coeficiente de realce (S= 10^2) e o fator de ganho (G = 10^2), gerando a imagem CEI (Equação 1). De maneira que as diferenças registradas entre períodos oscilam entre -1 e +1, em que os pixels com valores mais elevados apresentam maior probabilidade de representarem áreas cultivadas com soja.

Equação 1:

$$CEI = G * \frac{(MaxEVI+S)-(MinEVI+S)}{(MaxEVI+S)+(MinEVI+S)}$$

As metodologias CEI e CEI-PE apresentam algumas similaridades, ambas utilizam imagens EVI em dois períodos específicos a identificação da cultura da soja. Contudo, no período do MaxEVI ocorrem as diferenças em relação a metodologia CEI. De tal modo, foram utilizados os períodos entre os DA 321 a 48; 321 a 32 e 321 a 16, gerando as imagens MaxEVI-49, -33 e -17, respectivamente. Esta denominação tem origem na data posterior a última imagem EVI utilizada em sua composição. Ademais, a imagem CEI-PE recebe a identificação do MaxEVI utilizado, por exemplo, em CEI-49 foi utilizada a imagem de MaxEVI-49.

O passo seguinte é a classificação das imagens CEI-PE, quando foi definido um valor de limiar de fatiamento a partir do qual um pixel da imagem CEI-PE pertence à classe soja. De tal forma que foi utilizado um limiar diferente para cada estimativa prévia. Isto ocorre, para que o valor total de área de soja mapeada na safra 2005/2006, em nível estadual, seja similar em todas as abordagens. Para tanto, os valores de limiar apresentaram uma ordem, onde CEI-49>CEI-33>CEI-17, sendo todos inferiores ao valor utilizado em CEI original. Posteriormente, os mapas de CEI-PE receberam a aplicação de um filtro de moda com janela móvel de 5 x 5 pixels, tal qual ao utilizado na metodologia CEI original. Esta operação visa eliminar os pixels classificados ou não que se apresentam isolados nos mapas, oriundos provavelmente de ruídos nas imagens

MODIS.

A partir dos mapas de estimativa prévia obtidos com CEI-PE e do mapa de soja CEI original, foram gerados os mapas de comparação para cada estimativa prévia. Estes apresentam três classes temáticas, são elas acerto, omissão e inclusão. Em seguida, estes mapas foram confrontados a um mapa contendo os limites político-administrativos dos municípios analisados, de maneira a originar um novo mapa contendo a identificação dos municípios e das classes temáticas analisadas. Em seguida, para cada estimativa prévia, foi gerado um mapa de resultados, individualizando as classes temáticas acerto, omissão e inclusão. Neste caso, os pixels coincidentes nos mapas CEI-PE e CEI são definidos como acerto. Os pixels identificados como soja somente em CEI-PE são denominados de inclusão. Já aqueles identificados como soja somente em CEI pertencem à classe omissão. Cabe ressaltar ainda, que foi definido que todos os municípios com valores de acerto espacial acima de 90% apresentavam concordância mínima entre os mapas de soja CEI-PE e CEI. Foi definido este valor de concordância entre os mapas, como forma de tornar possível a utilização do CEI-PE como ferramenta de apoio a projetos operacionais, visto que uma metodologia precisa apontar as sua confiabilidade para se tornar útil aos possíveis usuários. Como exemplo de possíveis usuários desta ferramenta está a Moratória da soja e projetos de monitoramento de desmatamento. Para facilitar a interpretação dos resultados os mapas foram reclassificados em faixas de intervalos definidos, de maneira a agrupar as classes mais similares em um menor número de classes sem que ocorram prejuízos na análise destes mapas, (Fig. 2).

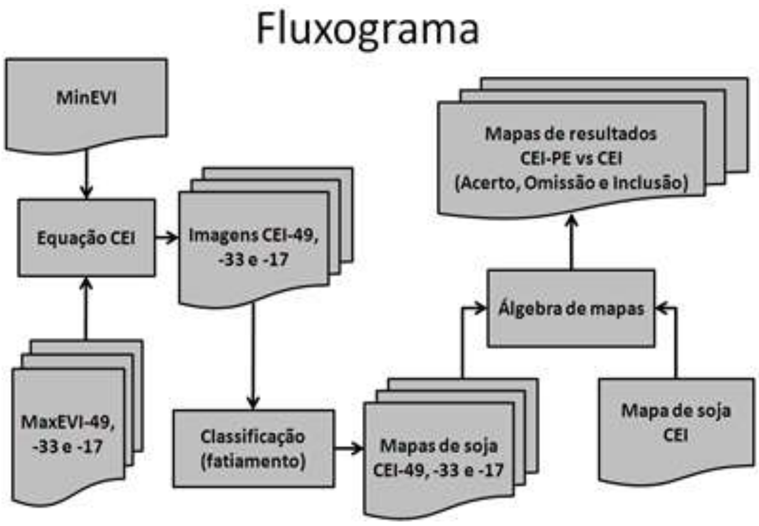

Fig. 2. Procedimento de análise espacial dos mapas gerados através da metodologia CEI- PE vs CEI, no MT para a safra 2005/2006

3. RESULTADOS E DISCUSSÃO

A estimativa CEI-49 apresentou o maior número de municípios (22 dos 42 analisados) com acerto acima de 90%. São eles: Comodoro, Tagará da Serra, Brasnorte, Porto dos Gaúchos, Campo Verde, Rondonópolis, Santo Antonio do Leste, General Carneiro, Querência, Diamantino, Tapurah, Ipiranga do Norte, Santa Rita do Trivelato, Vera, Nova Ubiratã, Jaciara, Campos de Júlio, Sapezal, Campo Novo dos Parecis, Nova Mutum, Sorriso e Lucas do Rio Verde. Em CEI-33, somente 7 municípios foram identificados com tal acerto espacial, sejam eles Sapezal, Campo Novo dos Parecis, Santa Rita do Trivelato, Campos de Júlio, Nova Mutum, Lucas do Rio Verde e Sorriso. Na estimativa CEI-17, somente os municípios de Nova Mutum, Sorriso e Lucas do Rio Verde alcançaram o valor de concordância mínima. Quando analisados em conjunto os municípios nos mapas de resultados contendo os acertos, observou-se que existem duas regiões com maior acerto espacial nas estimativas CEI-49 e -33, uma na porção oeste do MT nas circunvizinhanças de Sapezal e outra nos arredores do município de Sorriso. Entretanto, quando tratamos da estimativa CEI- 17, os maiores acertos estão concentrados somente na região de Sorriso (região em tons de verde na

Fig. 3). Ademais, estes municípios melhor identificados nesta estimativa apresentam tradição no cultivo de soja e não estão entre os municípios de expansão de fronteira agrícola. Estes fatos apontam para a possibilidade de existir uma maior sincronia e precocidade de plantio da cultura nesta região, de modo a possibilitar maiores acertos já em CEI-17.

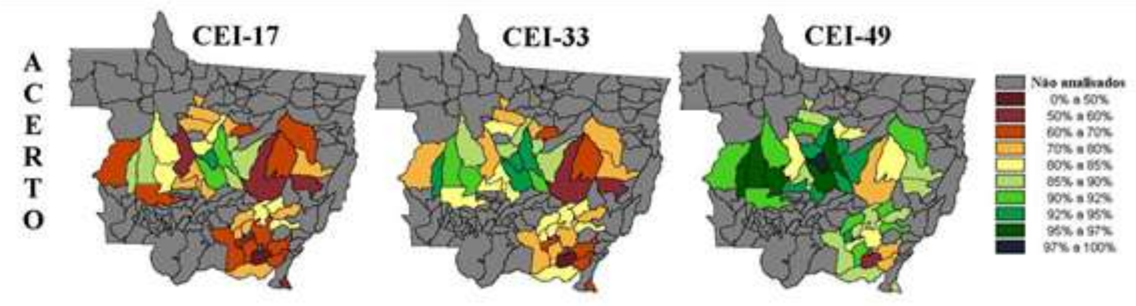

Fig. 3. Mapas de resultados para o acerto espacial, originados entre a Metodologia CEI-PE e CEI, para CEI -49, -33 e -17, para a safra 2005/2006.

Para a classe inclusão, na estimativa CEI-49 é possível constatar que a maioria dos municípios apresentou valores abaixo de 10%, com a distribuição destes erros mais homogênea nos 42 municípios analisados. Esse erro foi ainda menor (até 3%) para alguns dos principais municípios produtores de soja do Estado, tais como Campos de Júlio, Sapezal, Brasnorte, Campo Novo dos Parecis, Diamantino, São José do Rio Claro, Nova Mutum, Lucas do Rio Verde, Nova Ubiratã, Santo Antonio do Leste e Alto Taquari. Para CEI-33 e -17 ocorreu um aumento dos erros de inclusão, observando-se somente o município de Campos de Júlio com erro menor que 3%. Por outro lado, alguns municípios apresentarem valores de inclusão elevados mesmo em CEI-49, como o município de Pedra Preta, localizado na região Sul do MT. Este município sempre apresentou um dos maiores erros de inclusão entre todos os municípios nas três estimativas prévias e apresenta uma das menores áreas cultivadas com soja dentre os municípios analisados. Da mesma forma, a região sudeste do MT apresentou maiores erros de inclusão em relação ao restante do estado. Ademais, fica demonstrado que nos municípios analisados, podem existir um ou mais cultivos implantados durante com calendários agrícola similares ao da soja, que apresentam acréscimo de biomassa capazes de produzir valores de índice CEI-PE similares aos da soja (por exemplo, milheto utilizado como fonte de palha para o plantio direto do algodão no mês de novembro), gerando maiores erros de inclusão nas estimativas CEI-33 e -17. Esta ocorrência é menor em CEI-49 por conta da utilização de um valor de limiar mais elevado para a classificação nesta estimativa prévia, sendo este limiar mais próximo aquele utilizado em CEI original, de tal forma que os pixels assim classificados apresentam maior probabilidade de representar soja, fato este evidenciado pelo menor erro de inclusão registrado em CEI-49.

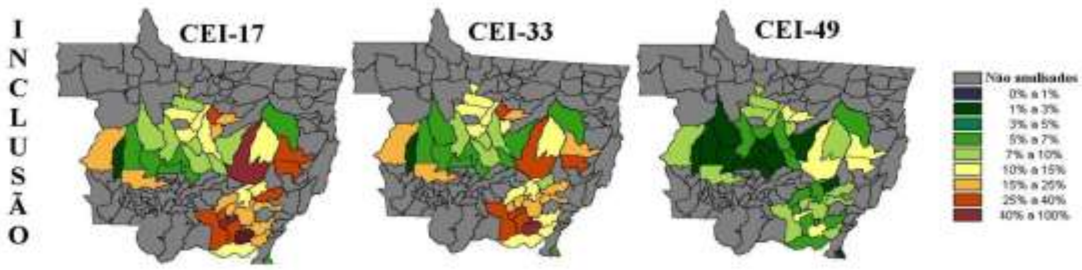

Fig. 4. Mapas de resultados para inclusão, originados entre a Metodologia CEI-PE e CEI, para CEI-49, -33 e -17, para a safra 2005/2006

Por fim, os resultados de omissão em CEI-49 demonstraram um número maior de municípios com erros abaixo de 3% (Fig. 5). Sendo eles Comodoro, Campos de Júlio, Nova Mutum, Ipiranga do Norte, Santa Rita do Trivelato, Vera, Nova Ubiratã, Jaciara, Tapurah, Lucas do Rio Verde e Sorriso. Para as estimativas CEI-33 e -17 foram observados com erros de omissão inferiores a 3%, respectivamente, quatro e dois municípios (Nova Mutum, Sorriso, Jaciara e Lucas do Rio Verde) e (Sorriso e Lucas do Rio Verde). Por outro lado, em CEI-17 evidenciaram-se municípios com elevados valores deste erro, como por exemplo, Alto Taquari e Nova Maringá que apresentaram 37% de omissão. Este fato pode estar associado a semeadura e/ou desenvolvimento mais tardio da soja em relação ao restante do Estado. Consequentemente, provocando aumento de omissão das áreas de soja à medida que reduz-se o período de composição do MaxEVI, de tal forma que as áreas cultivadas com soja ainda não apresentam valores de índice CEI dentro dos valores de limiar em CEI-33 e -17.

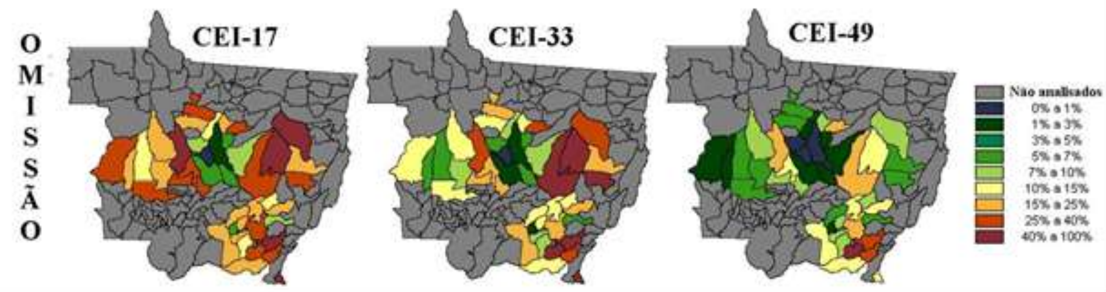

Fig. 5. Mapas de resultados para a omissão, originados entre a Metodologia CEI-PE e CEI, para CEI-49, -33 e -17, para a safra 2005/2006

Em suma, constata-se que alguns municípios apresentaram acerto espacial acima de 90% já em CEI-17, como por exemplo, Lucas do Rio Verde, Sorriso e Nova Mutum, tornando estes municípios passíveis de uma estimativa prévia mais confiável. Semelhantemente, estes municípios permaneceram entre aqueles de maior acerto também em CEI-49 e -33. Ademais, todos os municípios apresentaram maior acerto espacial em CEI-49 quando comparados a CEI-33, da mesma forma de CEI-33 quando comparados a CEI-17. Entretanto, outros municípios apresentaram valores de acerto acima dos 90% somente em CEI-49. Da mesma forma, os maiores valores de erro de inclusão e omissão foram identificados em municípios que representam menores percentuais da área cultivada. Ou seja, aparentemente existe uma relação positiva entre porcentagem de área cultivada por município e o acerto espacial nas estimativas prévias.

4. CONCLUSÃO

A cada estimativa prévia realizada através de CEI-PE, um mesmo município apresenta diferentes valores de acerto espacial na comparação com o mapa CEI. Assim, através de CEI- PE com mais de 90% de concordância com CEI foram identificados 22, sete e três dentre os 42 municípios estudados nas estimativas CEI-49, -33 e -17, respectivamente. De modo geral, em uma mesma estimativa prévia os municípios com maior área cultivada no estado apresentaram valores mais elevados de acerto espacial em relação aqueles de menor área cultivada. Para cada um dos 42 municípios analisados, quando comparados individualmente nas três estimativas prévias, sempre ocorreram maiores valores de acertos em CEI-49, decrescendo até CE-17. Entretanto, alguns municípios não apresentam um valor de acerto espacial elevado nem mesmo em CEI-49. Ademais, os erros de omissão foram maiores que os de inclusão para a maioria dos municípios nas três estimativas prévias. Com alguns municípios apresentando elevados erros de inclusão ou omissão em CEI-49.

Por outro lado, identificaram-se alguns municípios com acertos espaciais acima de 90% de quando comparados ao mapa de referência já em CEI-17. Entretanto, a maioria dos municípios foi identificada com maior acerto somente em CEI-49, e ainda, com uma ordem decrescente de acerto espacial de CEI-49 a -17. Deste modo, evidenciando que para estes municípios com menor acerto espacial as imagens EVI adquirida entre os DA 49 e 64 são cruciais para a correta identificação das áreas de soja.

6. REFERÊNCIAS

Asner, G. P. Cloud cover in Landsat observations of the Brazilian Amazon. International Journal of Remote Sensing,

vol. 22, no. 18, 3855–3862, 2001.
CONAB – Companhia Nacional de Abastecimento. Acompanhamento Acompanhamento de safra brasileira: grãos, décimo levantamento, julho 2011. Brasília: Conab, 2011. Disponível em: http: //www.conab.gov.br/OlalaCMS/uploads/arquivos/11_07_15_11_3_18_boletim_julho_2011..pdf >. Acesso: 28 mar. 2012.
CONAB – Companhia Nacional de Abastecimento. Valores das exportações do complexo soja. Disponível em: <http:www.conab.gov.br/conteudos.php?a=546&t=2> Acesso: 30 mar. 2012.
Didan, K.; Huete, A. R. MODIS Vegetation Index product series Collection 5 change summary. The University of Arizona. Arizona. Jun., 2006. Disponível em: <http://landweb.nascom.nasa.gov/QA_WWW/forPage/MOD13_VI_C5_Changes_Document_06_28_06. pdf >.
Huete, A.; Liu, H. Q.; Batchily, K.; Leeuwen, W. A comparison of vegetation indices over a global set of TM images for EOS-MODIS. Remote Sensing of Environment, n. 59, p. 440–451, 1997.
Huete, A.; Justice, C.; Leeuwen, W. V. Modis vegetation index (MOD 13) algorithm theoretical basis document, 1999. Disponível em: <modis.gsfc.nasa.gov/ data/atbd /atbd_mod13.pdf>. Acesso em: 21 mar.2012.
IBGE - Instituto Brasileiro de Geografia e Estatística. Relatórios metodológicos.Pesquisas agropecuárias/IBGE, Departamento de Agropecuária. 2ª ed. Rio de Janeiro, 2002, 92 p. Disponível em: <http:// www.ibge.gov.br/home/estatistica/indicadores/agropecuaria/PesquisasAgropecuarias2002.pdf >. Acesso em: 15 ago. 2012.
IBGE – Instituto Brasileiro de Geografia e Estatística. Banco de Dados Agregados, Sistema IBGE de Recuperação Automática SIDRA. 2010b Disponível em: <http://www. sidra.ibge.gov.br/bda/tabela/protabl.asp?c=1612&z=p&o=24&i=P>. Acesso em: 24 ago. 2012.
Eberhardt, I. D. R.; Rizzi, R.; Risso, J.; Fernandes, S. L. Identificação prévia das áreas de soja por meio da metodologia CEI em imagens MODIS. Congresso de Iniciação Científica (CIC), Anais do CIC, Pelotas, Brasil, 2011.
Justice, C. O.; Vermote, E.; Townshend, R.; Defries, R.; Roy, D. P.; Hall, D. K.; Salomonson, V. V.; Privette, J. L.; Riggs, G.; Strahler, A.; Lucht, W.; Mynemi, R. B.; Knyazikhin, Y.; Running, S. W.; Nemani, R. R.; Wan, Z.; Huete, A. R.; Leeuwen, W. V.; Wolfe, R. E.; Giglio, L.; Muller, J. P.; Lewis, P.; Barnsley, M. J. The Moderate Resolution Imaging Spectroradiometer (MODIS): Land Remote Sensing for Global Change Research. IEEE TRANSACTIONS ON GEOSCIENCE AND REMOTE SENSING, VOL. 36, NO. 4, p.1228-1249, JULY 1998.
Leeuwen, W. D.; Huete, A. R.; Laing, T. W. MODIS Vegetation Index Compositing Approach: A prototype with AVHRR data. Remote Sensing of Environment, n. 69, p. 264–280, 1999.
MDIC - Ministério do Desenvolvimento, Indústria e Comércio Exterior. Departamento de Planejamento e Desenvolvimento do Comércio Exterior - DEPLA, da Secretaria de Comércio Exterior – SECEX. Conhecendo o Brasil em números. Brasília. Disponível em:< www.mdic.gov.br//arquivos/dwnl_1289222248.pdf>. Acesso em: 20 mar. 2012.
Pino, F. A. Estatísticas agrícolas para o século XXI. Agric. São Paulo, SP, 46(2): 71-105, 1999.
Pino, F. A. Estimação subjetiva de safras agrícolas. Informações Econômicas, SP, v.31, n. 6, jun., 2001.
Rizzi, R.; RUDORFF, B. F. T. Estimativa da área de soja no Rio Grande do Sul por meio de imagens Landsat. Revista Brasileira de Cartografia, v.57, p.226-234, 2005.
Rizzi, R.; Risso, J.; Epiphanio, R. D. V.; Rudorff, B. F. T.; Formaggio, A. R.; Shimabukuro, Y. E.; Fernandes, S. L. Estimativa da área de soja no Mato Grosso por meio de imagens MODIS. Anais do XIV SBSR. Natal. INPE p.387-394, 2009. Disponível em:< http://marte.dpi.inpe.br/col/dpi.inpe.br/sbsr@80/2008/11.16.18 .50.57/doc/387-394.pdf>. Acesso em: 20 mar. 2012.
Rudorff, B. F. T.; Berka, L. M. S.; Moreira, M. A.; Duarte, V.; Xavier, A. C.; Rosa, V. G. C.; Shimabukuro, Y. E. Imagens de satélite no mapeamento e estimativa de área de cana em São Paulo: ano-safra 2003/04. Agricultura São Paulo, São Paulo, v.52, n.1, p.21-39, 2005.
Rudorff, B.F.T.; Adami, M.; Risso, J.; Aguiar, D.A.; Pires, B.; Amaral, D.; Fabiani, L.; Cecarelli, I. Remote Sensing Images to Detect Soy Plantations in the Amazon Biome—The Soy Moratorium Initiative: Sustainability, v.4, p.1074-1088, 2012.
USDA – United States Departament of Agriculture. Foreign Agricultural Service. Oils seeds: World markets and trade. Circular series, FOP 11-12, Dec. 2011. Disponível em: <http://www.Fas.usda.gov/oilseeds/circular/2011/Dec/oilseeds_full12-11pdf>Acesso em: 20 jul. 2012.

Mud banks, sand flux and beach morphodynamics in French Guiana: A remote sensing approach

Edward Anthony 1*; Antoine Gardel 2; Franck Dolique 3; Andy Chatelet 1; Christina Péron 5**; Benjamin Kulling 1and Guillaume Brunier 1**

1 Aix Marseille Université, CEREGE, UMR CNRS 7330, Europôle de l'Arbois, B.P. 80, 13545 Provence Cedex, France
2. Université du Littoral Côte d'Opale, Laboratoire d'Océanologie et de Géosciences,
3. Université Antilles-Guyane, Campus de Martinique,
*Institut Universitaire de France, **CNRS Guyane,
anthony@cerege.fr

ABSTRACT

Sandy beaches affected by mud in an open-coast, wave-dominated setting are rare. Using aerial photographs from the 1950s and satellite images from 1986, beaches on the muddy, Amazon-influenced coast of French Guiana have been classified into three categories, each with a characteristic morphodynamic pattern: (1) short embayed pocket beaches (0.1-1 km-long), (2) longer (>2< 5 km-long) more open beaches between bedrock headlands, and (3) open, non-embayed chenier beaches. Beach morphodynamics are essentially controlled by alternations between phases when mud banks migrating northwestwards from the mouth of the Amazon River attain French Guiana, leading to mud-mound beaches associated with virtually total wave energy dissipation, and 'inter-bank' phases characterised by relative scarcity of mud, enhanced wave activity and 'normal' beach morphodynamics. As type 1 beaches are strongly constrained by headlands, their dynamics during inter-bank phases involve essentially cross-shore sand mobility. Type 2 beaches are less constrained and undergo a process of 'rotation', involving active longshore sand fluxes that generate periodic alternations in erosion and recovery at the two ends of the beach under a globally balanced sand budget. Type 3 beaches are cheniers generally formed in the vicinity of river mouths under the strong influence of a 'hydraulic-groyne' effect in which estuarine liquid discharge favours mud liquefaction and sandy deposition. The remote sensing data highlight marked differences in the timing and intensity of mud-bank and inter-bank phases, a problem in terms of beach management in the rapidly developing context of French Guiana.

Keywords: Muddy beach, Beach rotation, Amazon mud banks, Remote sensing, French Guiana

1. INTRODUCTION

Intertidal beaches affected periodically or permanently by mud on wave-dominated coasts are extremely rare, because of hydrodynamically controlled non-deposition of mud, and the common lack of substantial nearby mud supplies. Generally, sandy beaches evolve alongshore into muddy tidal flats as a function of wave energy. Where mud supplies are important, this longshore energy segregation may also occur across shore with low-tide mud fronting a high- tide sandy beach. The influence of mud on sandy beaches has, however, elicited little interest in the literature, no doubt because of the rarity evoked above. Where abundant mud supplies occur, their effect on sandy beaches is generally vested in varying degrees of dissipation of wave energy. This dissipation can range from partial to total. In the former case, this can induce longshore and cross-shore variations in sand flux and the ensuing beach morphodynamics, and in the latter case, in no sand flux. Fine examples of mud-affected sandy beaches in an open-coast, wave-dominated setting occur in French Guiana, which lies on the world's longest muddy coast between the mouths of the Amazon and the Orinoco Rivers (Figure 1). Using a remote-sensing approach, we identify the various beach types in this muddy setting, and show the joint influence of the local geomorphic context and of mud from the Amazon on sand fluxes and, hence, the morphodynamics of these beaches.

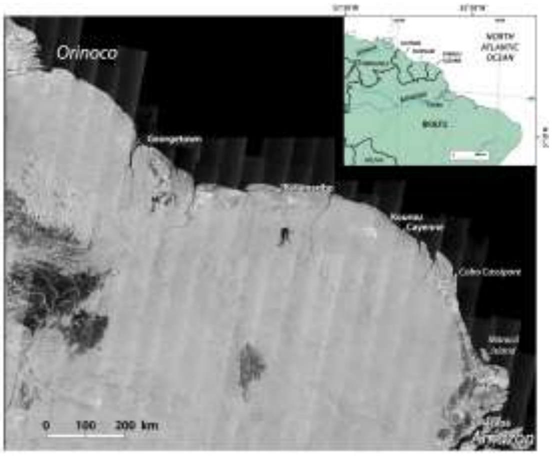

Figure 1. The general setting of the French Guiana coast in an ALOS 2007 satellite image showing the muddy coast of South America between the Amazon and the Orinoco river mouths

2. REGIONAL SETTING AND METHODS

The sedimentary geology and morphodynamics of the coast of South America between the mouths of the Amazon and the Orinoco are dominated by the massive fine-grained sediment discharge of the Amazon. The influence of the Amazon is essentially imprinted via a unique system of successive mud banks that circulate alongshore. The dynamics of these banks and their interactions with the shoreline have been recently reviewed by Anthony et al. (2010). Each mud bank can be up to 60 km-long and 30 km-wide, and can contain several times the annual mud supply of the Amazon (ca. 750-1000 million tonnes per annum (Martinez et al., 2009)). In this Amazon-dominated coastal environment, one of the muddiest in the world, sandy beaches are rare, and generally form cheniers, and in French Guiana, headlound-bound bay beaches in Cayenne and Kourou (Figure 1). The beaches in French Guiana are characterised by relatively uniform coarse to fine quartz sand, a variable amount of heavy minerals and a very small fraction (<1%) of shelly debris. These sandy beaches, of limited length, are important both economically and ecologically on this muddy coast because they provide locations for human settlement and routes. The rare beaches on this part of the South American coast are also important for the successful nesting and ecology of protected marine turtles (*Lepidochelys olivacea*, *Chelonia mydas*, *Eretmochelys imbricata*, *Dermochelys coriacea*). The sandy beaches of Cayenne offer rare recreational space and egg-laying sites for marine turtles for over 300 kilometres of muddy shore west of the mouth of the Amazon (Figure 1).

French Guiana beaches are affected by trade winds from the northeast that are mainly active from January to April. Waves have periods ranging from 6 to 12 s, indicating a mix of trade wind-waves and longer swell, while offshore modal heights are up to 1.5 m. The longer-period swell waves (> 10 s) are generated by North Atlantic depressions in autumn and winter and by Central Atlantic cyclones in summer and autumn. The most energetic trade wind-waves are observed between January and April in response to peak wind activity while swell waves appear to be most frequent in autumn and winter, reinforcing the relatively high winter to early spring wave-energy regime induced by the trade winds. Tides are semi-diurnal and the spring tidal range is mesotidal (2.5 to 3.1 m).

The longshore migration of the mud banks, essentially under the influence of waves (Gardel and Gratiot, 2005; Gratiot et al., 2007, 2008), results in marked space- and time-varying coastal geomorphic changes that can be summarized in terms of alongshore-alternating 'bank' and 'inter-bank' zones (Anthony and Dolique, 2004). Differences in migration rates also account, in part, for variations in the spacing between the banks, and possibly bank morphology as well, notably where mud banks are 'stretched' alongshore. Banks and their mangrove vegetation dissipate wave energy, protecting the coast from wave attack. Inter-bank areas between the dissipative mud banks are associated with a deeper shoreface. They are either subject to rapid shoreline retreat (Anthony *et al*., 2011) over timescales corresponding to the inter-bank phases (order of years) where the coast has previously accreted through mud bank 'welding' onshore, or exhibit, where sandy beaches are present, typical beach morphodynamic behaviour.

The French Guiana beaches have been monitored using a multi-scale approach involving remote sensing, observations from low-flying aircraft and field measurements. The overall database covering these sources involves 60 years of coverage provided by aerial photographs and 26 years of SPOT satellite images. Given the time frame of beach change under the influence of the large migrating mud banks (migration rates of the order of 1-5 km/yr), such long-term time series of remote sensing data are important in attempting to characterise the morphodynamics of beaches in this muddy context and to decipher ensuing cycles of beach change.

3. RESULTS AND DISCUSSION

Beaches in French Guiana fall into three categories: (1) highly embayed short pocket beaches (0.1-1 km-long), locally referred to as *anses* (literally small bays), (2) longer (>2< 5 km-long) more open beaches between bedrock headlands, and (3) open, non-embayed chenier beaches. Type 1 beaches are limited to the bedrock promontories of Cayenne and Kourou (Figure 1), the hard-rock headlands of which consist of migmatites and granulites. The longer embayed type 2 beaches are located exclusively in Cayenne. The embayments between these headlands are bound by narrow (<500 m) sandy fringing beaches that generally abut older, probably Pleistocene, deposits that form a stiff, widespread reddish clay deposit. Locally, pronounced beach erosion may lead to exposure of these deposits in the backshore area. Type 3 chenier beaches are generally formed in the vicinity of river mouths. Cheniers are poorly developed in French Guiana, probably because the debouching rivers are small, and, therefore, the sand supply to be expected from these rivers rather limited, and significantly blanketed by mud from the nearby Amazon which dominates the coastal progradational regime (Anthony et al., in press).

3.1. Type 1 beaches

The numerous small type 1 pocket beaches of Cayenne and Kourou are particularly prone to prolonged trapping of mud, because of their commonly highly embayed plan shape, even during transitional phases (Dolique and Anthony, 2005). As a result of the prolonged protection offered by mud in these embayed settings, changes in upper beach morphology are rather mild, even during inter-bank phases. However, on all pocket beaches, transitional and inter-bank phases are characterized by an increase in incident wave breaker heights that goes apace with erosion of subsisting mud inshore and lowering of the muddy low-tide surface. During these phases, sand released by seasonal erosion of the upper beach is transported offshore, forming diffuse sand blankets overlying mud. During the low-energy season, this sand is washed out of the muddy profile and transported back up the beach. The recovery trend is thus characterized by seasonal beach behaviour. As the full inter-bank phase occurs, more significant erosion of mud by larger incoming waves leads to an important seaward relocation of the mud-sand contact. Observations of the overall beach morphology suggest that the temporal profile variability of these pocket beaches basically involves fluctuations in the level of the lower beach mud surface and mild cross-shore sand movements. The profile changes and the morphology suggest little longshore movement of sand.

3.2. Type 2 beaches

Four SPOT images corresponding to the years 1986, 1995, 2003 and 2011 summarize the general medium-term dynamics of the three type 2 beaches in Cayenne (Figure 2). The situation in Figure 2a corresponds to a 'bank' phase in 1986. In this situation, mud has welded directly onshore, but the image does show the presence of a sandy beach only in the southeastern sectors of Montjoly and Remire beaches, thus suggesting erosion or fossilisation of the beaches in the northwestern sectors of both beaches by the important muddy foreshore which is up to 1 km-wide. The image follows at least two years of complete mud-bounding and mangrove colonization of the mud, and shows the inception of mud erosion, especially in the southeastern sector of Montjoly and of the neighbouring Rémire beach. Within the ten- year interval between the 1986 and 1995 images, the return to an inter-bank phase had resulted in complete erosion of the welded part of the mud bank and the instauration of 'normal' wave-beach interactions. The 1995 image

(Figure 2b) shows the recovery of the beaches and fairly balanced beach widths. The 2003 image (Figure 2c) corresponds to a new bank phase. Unlike the 1986 situation where all the beaches of Cayenne were completely mud-bound (Figure 2a), the 2003 situation was one of partial mud welding on the main Cayenne beaches, with welding becoming much more significant on just the western part of the Cayenne promontory, notably covering Montabo beach. The image shows an eroded Montjoly beach bound by a significant patch of mud. The 2011 image shows a full inter-bank phase and the remarkable recovery of the beaches, with abundant sand accumulation in the northwestern sector of Montjoly beach (yellow box in Figure 2d).

3.3 Type beaches

Cheniers are important on this muddy coast as, in addition to serving as settlement areas and providing coast-parallel routes, they protect low-lying inland areas against flooding. These beaches consist of local concentrations of fine to coarse quartz sand winnowed out from subtidal mud (Figure 3). This sand is generally supplied by the local rivers, or derived from the reworking of older, fossil cheniers inland that are attacked during phases of severe inter- bank erosion. As cheniers develop and gain volume, they sometimes provide a continuous alongshore pathway for sand transport, punctuated by washover zones that may lead to their dismantling. Strong alongshore gradients in sand drift are thus generally observed during chenier formation. In Surinam and Guyana, however, where larger rivers debouching on the coast have supplied sand, significant bands of cheniers have been incorporated in the prograded muddy coastal plain.

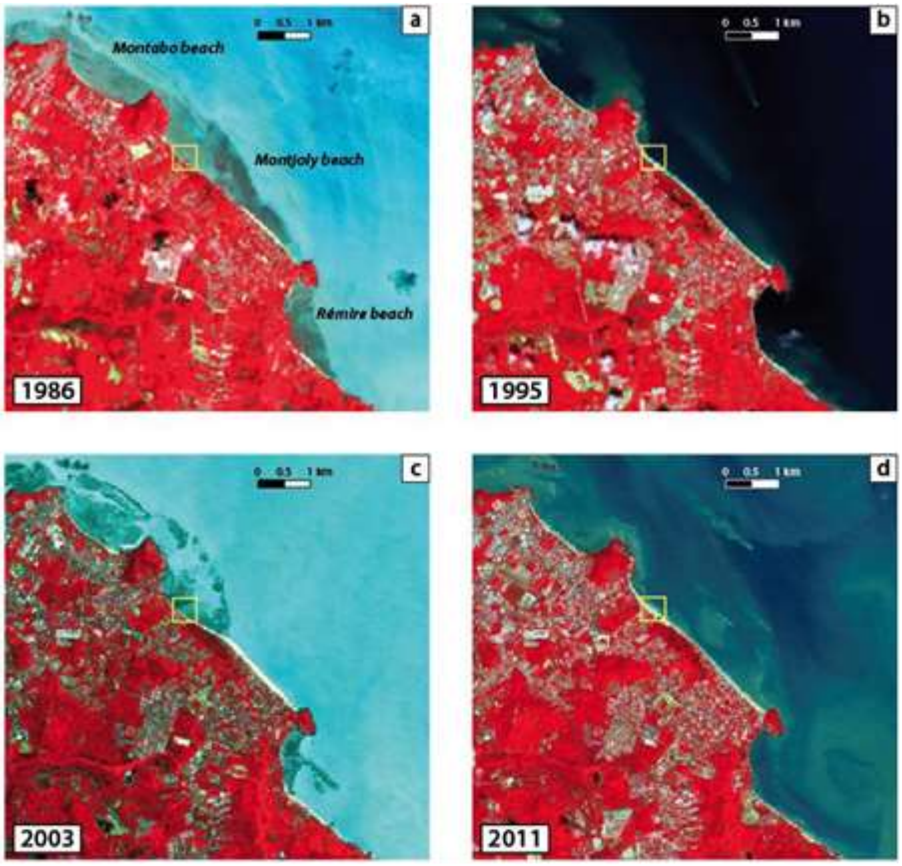

Figure 2. Four SPOT images showing changes in embayed, headland-bound type 2 beaches on the Cayenne promontory associated with bank and inter-bank dynamics: (a) bank phase in 1986 resulting in completely mud-bound beaches; (b) inter-bank phase in 1996 and the instauration of 'normal' wave-beach interactions; (c) bank phase in 2003 but with only partial welding of mud on beaches that had earlier undergone marked erosion in their northwestern sectors; (d) inter-bank phase in 2011. Yellow box highlights zone of clear changes in beach width that are a signature of beach rotation (see text for explanation)

The liquid discharge of these Guiana Shield rivers appears to induce a ‘hydraulic-groyne’ effect on mud-bank translation alongshore that needs to be taken into account in the analysis of chenier formation (Anthony et al., in press). This hydraulic-groyne effect may be responsible for more persistent muddy accretion on coastal sectors updrift of these large river mouths by slowing down mud-bank migration and encouraging mud concentration. A corollary of this is associated hindered muddy sedimentation downdrift of the river mouths due to significant offshore deflection of mud banks in transit alongshore. These differences can be quite marked on either side of these river mouths due to this ‘groyne’ effect. Downdrift mud deficit induced by this effect may go hand in hand with the more common sandy chenier formation exhibited by the downdrift sectors of the coast, as seen on either side of the Maroni on the French Guiana-Surinam border.

Figure 3. Oblique aerial photograph showing a set of sandy cheniers in western French Guiana

At the largest spatio-temporal scale, the morphodynamics of the three beach types in French Guiana is essentially controlled by interactions between waves and the massive mud banks that dissipate wave energy as they migrate alongshore at rates of a few kilometres a year. Since these banks are separated by mud-deficient inter-bank zones associated with a much less dissipative inner shoreface, such inter-bank zones (and inter-bank phases) are the loci of sand concentration within this predominantly muddy environment. The presence of mud significantly alters the behavioural patterns of beaches on this muddy coast, which is normally influenced by seasonal changes in wave energy due to trade-wind activity. The aerial photographs clearly show that the chief effect of mud banks on the morphodynamics of type 2 beaches is periodic alternations in longshore drift that lead to a rare form of beach rotation that does not result from variations in deepwater wave approach directions, as is generally reported for non-mud bank-affected beaches (e.g., Thomas et al., 2010). In the case of the French Guiana beaches, beach rotation is a medium-term (order of a few years) process due to changes in shallow shoreface bathymetry induced by the migrating subtidal to intertidal mud banks. These bathymetric changes affect wave refraction and dissipation patterns, resulting in marked longshore gradients in incident wave energy. These strong wave energy gradients along sections of the shore facing the leading or trailing edges of the mud banks generate lateral movement of sand in these headland-bound beaches, resulting in alternations in erosion and accretion over time, without net sediment loss. Illegal sand extractions, however, might finally endanger this equilibrium. These beach morphological changes have been defined in terms of a simple, four-stage conceptual model comprising bank, inter-bank and two transitional phases (Figure 4).

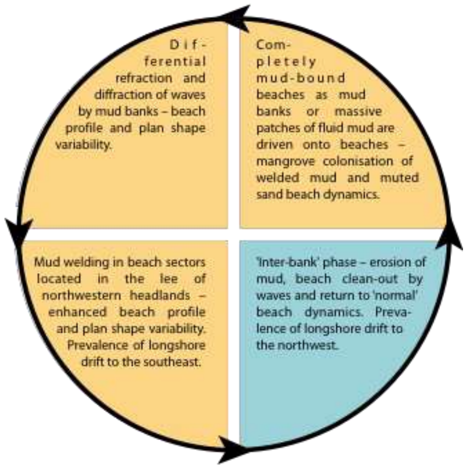

Figure 4. A four-phase model of sandy beach morphological change involving rotation of type 2 beaches in Cayenne, French Guiana, in response to Amazon mud-bank activity. The cycle comprises a bank, an inter-bank and two transitional phases, as a typical mud bank attains and migrates past the Cayenne promontory. The transitional phase between bank and inter-bank phases shows the most rapid (days to months) and most spectacular beach changes because the natural longshore drift (from southeast to northwest) generated by trade-wind waves on this coast is reinforced by longshore gradients in wave height due to inshore dissipation by mud trapped by northwestern headlands. This occurs as the trailing edge of a mud bank goes past each headland-bound beach in Cayenne. Modified, from Anthony and Dolique, 2006

The short, type 1 mud-affected pocket beaches do not show the rotational response of the longer open beaches. In these highly embayed pocket beaches, this situation is due to both the more limited sand accommodation space which goes with a lower overall beach volume, and marked refraction of waves. Due to the short length of these pocket beaches, longshore wave energy gradients generated by variations in the nearshore mud cover cannot develop properly. Beach plan-shape morphological changes are therefore much less spectacular than those affecting the longer beaches. Changes are essentially cross-shore, involving profile erosion and trapping of sand within the inshore mud prism and recovery during the low-energy season. This seasonal frame of beach morphological change occurs essentially during the inter-bank phase, as these short pocket beaches can be significantly mud-bound even during the transitional phases.

While the model of evolution of type 2 beaches is inscribed in a cycle of rotation, there is presently no certainty as regards cycle duration. Each bank-to-bank cycle apparently involves periods of several years, certainly exceeding a decade. The 60-year aerial photographic coverage suggests mesoscale cycles of 10 to 20 years. The SPOT image coverage depicted in Figure 2 suggests a cycle of 17 years between the 1986 and 2003 bank phases. However, this periodicity involves several uncertainties and the two bank phases are quite dissimilar, the 2003 one being only partial, and, thus, conducive to strong longshore gradients in sediment flux. Apart from this condition of the degree of mud-bounding, the duration of this accumulation limb of the bank-to-inter-bank cycle is totally dependent on the rate at which the next bank intrudes on the beaches of Cayenne. In the present cycle, this duration has now attained 10 years (2002-2012), and will be interrupted in the next two years given the proximity of the next incoming mud bank. This heralds the onset of a new cycle of sand flux towards the southeast on both Montjoly and Rémire beaches under an impending bank phase. This phase will ultimately induce a new beach rotation cycle involving the erosion of the northwestern sector of Montjoly beach adjacent to the lagoon, as in 1998-2000. Gratiot et al. (2007) noted a poor correlation between wave forcing and migration rates because of the contribution of other mechanisms to bank migration, such as local morphology. Regarding type 3 chenier beaches, there is also a need for a better comprehension of Guiana Shield sand inputs to the coast and of river-mouth dynamics in their development, especially as regards the interaction between the river-mouth hydraulic jet and mud banks migrating alongshore.

4. CONCLUSIONS

Sandy beaches in French Guiana are important in terms of coastal zone management and ecology. Three beach types have been defined from aerial photographs and satellite images, which have provided long-term remote sensing data for analysing beach morphodynamic patterns on this muddy coast. The morphology and behaviour of these beaches are controlled by their local morphological context as well as by mud-bank and inter-bank phases that determine levels of wave-energy dissipation. Type 1 pocket beaches show little longshore mobility while longer type 2 beaches between bedrock headlands in Cayenne are subject to periodic beach rotation, the time frame of which appears to be irregular, dependent on mud- bank size and migration rates. The formation and maintenance of type 3 chenier beaches are associated with estuary-mouth interactions with the migrating mud banks. These interactions require further studies.

5. REFERENCES

Anthony, E.J.; Dolique, F. The influence of Amazon-derived mud banks on the morphology of sandy, headland- bound beaches in Cayenne, French Guiana: A short- to long-term perspective. Marine Geology, v. 208, p. 249-264, 2004.

Anthony, E.J.; Gardel, A.; Dolique, F.; Marin, D. The Amazon-influenced mud-bank coast of South America: short- to long-term morphodynamics of ‘inter-bank’ areas and chenier development. Journal of Coastal Research, Special Issue 64, p. 25-29, 2011.

Anthony, E.J.; Gardel, A.; Gratiot, N.; Proisy, C.; Allison, M.A.; Dolique, F.; Fromard, F., 2010. The Amazon- influenced muddy coast of South America: A review of mud-bank-shoreline interactions. Earth-Science Reviews, v. 103, p. 99-121.

Anthony, E.J.; Gardel, A.; Proisy, P.; Fromard, F.; Gensac, E.; Peron, C.; Walcker, R.; Lesourd, S.; The role of fluvial sediment supply and river-mouth hydrology in the dynamics of the muddy, Amazon-dominated Amapá- Guianas coast, South America: a 3-point research agenda. Journal of South American Earth Sciences, in press, doi.org/10.1016/j.jsames.2012.06.005.

Gardel, A.; Gratiot, N. A satellite image-based method for estimating rates of mud banks migration, French Guiana, South America. Journal of Coastal Research, v. 21, p. 720-728, 2005.

Gratiot, N.; Anthony, E.J.; Gardel, A.; Gaucherel, C.; Proisy, C.; Wells, J.T. Significant contribution of the 18.6 year tidal cycle to regional coastal changes. Nature Geoscience, vol. 1, p. 169-172, 2008.

Gratiot, N.; Gardel, A.; Anthony, E.J. Trade-wind waves and mud dynamics on the French Guiana coast, South America: input from ERA-40 wave data and field investigations. Marine Geology, v. 236, p. 15-26, 2007. Martinez, J.M.; Guyot, J.L.; Filizola, N.; Sondag, F. Increase in sediment discharge of the Amazon River assessed by monitoring network and satellite data. Catena, vol. 79, p. 257-264, 2009.

Thomas, T., Philips, M.R., Williams, A.T. Mesoscale evolution of a headland bay: Beach rotation processes. Geomorphology, vol. 123, p. 129-149, 2010

Ocean color remote sensing in coastal waters of French Guiana: application of the ANR GlobCoast project

V. Vantrepotte; H. Loisel; X. Mériaux; D. Dessailly; A. Gardel and E. Gensac

INSU-CNRS, UMR 8187, LOG, Laboratoire d'Océanologie et des Géosciences, Université Lille Nord de France, ULCO, 32 avenue Foch, 62930 Wimereux, France

ABSTRACT

Remote sensing data now allow for an accurate description of a variety of physical and biological parameters at global scale with a temporal resolution hardly available from other measurement methods. The ANR GlobCoast first objective is to analyze, for the first time, the seasonal, interannual and decadal variability of the global coastal waters in term of biogeochemical composition using various descriptors available from ocean color remote sensing (i.e. Chlorophyll a, suspended particulate matter, dissolved and particulate organic carbon concentration). In the frame of GlobCoast, the latter parameters will be, in a first step, assessed through innovative approaches allowing to face the challenge represented by the development of inversion algorithms in optically complex waters such as the coastal waters. In the second step, time series for the latter biogeochemical parameters will be analyzed conjointly with various physical forcing parameters as obtained from remote sensing (wind, sea surface temperature, altimetry), in situ measurements, and modelling outputs. French Guiana coastal waters represent one of the coastal domains that will be particularly investigated in the context of GlobCoast. First results have emphasized the interest of classifying these coastal waters for better characterizing of the dynamics of French Guiana coastal ecosystems and potentially improving the accuracy of the SPM retrieval from space. Further, the analysis of the SPM time series computed for the MODIS archive over the French Guiana coastal domain has allowed to characterize the dynamics of local geomorphological processes (mud banks migration) and regional hydrodynamical forcings (north Brazilian retroflection current) on these coastal waters.

Keywords: ocean color, coastal waters, French Guiana, ANR-GlobCoast .

1. INTRODUCTION

Knowing that coastal areas concentrate about 60% of the world's population (within 100 km from the coast), that 75-90% of the global sink of suspended river load takes place in coastal waters in which about 15% of the primary production occurs, the societal and economical benefits of this project are potentially huge: fish resources, aquaculture, water quality information, recreation areas management, etc. Large uncertainties remain on the evaluation of the stocks of the main biogeochemical parameters in coastal waters and their seasonal, inter-annual, and decadal evolutions. In that context, satellite Remote Sensing of ocean colour is a very powerful tool for the management of resources and activities of continental shelf waters. However, the exploitation of these data in such a complex environment, where the optical properties do not necessarily covary with phytoplankton, requires the development of specific inverse methods to assess the required bio-optical and biogeochemical parameters. While some recent progress has been achieved, challenges still remain (IOCCG, 2000, 2006).
The French national ANR GlobCoast project (ANR Blanc, 2011-2013, http://www.foresea.fr/globcoast/, Partners: LOG, ULCO-Wimereux, GET-Toulouse, LEGOS- Toulouse, Hygeos-Lille) has been built in that context and is based on three main objectives.

The first one is to assess and analyse the seasonal, year-to-year, and decadal evolution of the global coastal waters in terms of biogeochemical composition as revealed from satellite ocean colour observations, for the very first time. Basic (inherent optical properties, chlorophyll a, as a proxy for phytoplankton biomass and suspended particulate matter concentrations) as well as more innovative products (particulate and dissolved organic carbon) will be assessed from new approaches developed in the frame of GlobCoast.

In the second part of the project, time series for the latter biogeochemical parameters will be analysed conjointly with various physical forcing parameters as obtained from remote sensing (wind, sea surface temperature, altimetry), in situ measurements, and modelling. This will help to gain a better understanding of the origins of the temporal variability of biogeochemical parameters over the coastal ocean. This part will be performed over highly contrasted areas covering a great variety of environmental, biological and bio-optical conditions encountered in coastal areas.

The third main objective of this project is to analyse the potential link between the variability of the environmental parameters as assessed in the first parts of the project, and the variance in the recruitment and stocks of higher trophic level organisms (i.e. fishes). While fishing pressure has a strong impact on recruitment and stocks, the contribution of environmental fluctuations to the variability in recruitment is now clearly demonstrated, especially thanks to remotely sensed data from satellite.

The achievement of the different objectives proposed in the frame of GlobCoast will hopefully lead to a better understanding of coastal biogeochemical cycles, and their relationship with physical forcing occurring in coastal areas, and the evolution of productivity and fish resources. The results of this project obtained over the global coastal ocean and over long-term observations, could help to distinguish non-systematic natural variability from trends and regime shifts in coastal ecosystems that have often been related to eutrophication or anthropogenic disturbances. In the same way, the spatio-temporal scales considered in this project, as well as the diversity of the data, will facilitate the assessment of the role of environmental conditions in the variability of stocks and recruitments of fishes. The data set generated in this project from ocean colour satellite observations is also of great interest for the validation of coupled biogeochemical-physical models designed for coastal waters. Significant discrepancies still remain between models and observations, and a number of key processes are still poorly quantified. The chlorophyll (Chl), suspended particulate matter (SPM), and particulate (POC) and dissolved (DOC) organic carbon products are particularly relevant for such models especially through the use of assimilation schemes.

French Guiana (and more largely regions influenced by the Amazon river outputs) coastal waters represent one of the coastal domains that will be specifically investigated in the context of GlobCoast especially regarding the two first objectives of this project. This coastal area which is one of the most dynamic coast in the world, especially due to the influence of the immense discharge of the Amazon river, which influences on the biogeochemical cycles and ecosystems functioning over the whole Guianese coastal area still remain to be better constrained. This works aims to present some of the applications that will be developed in the context of GlobCoast over the the French Guiana coastal waters illustrated in the present paper through first results obtained within this coastal region.

2. METHODS

2.1 Inversion of ocean color products from a classification-based approach

The development of inversion algorithms needed for relating satellite radiometric measurement to bio-optical (IOPs: particulate backscattering coefficient, b_{bp}, its spectral slope, g, or other descriptive parameters of the flocsize distribution, the absorption coefficients of phytoplankton, dissolved and non algal particles a_{phy}, a_{cdom}, and a_{nap}, respectively, diffuse attenuation coefficient K_d) and biogeochemical (e.g. Chlorophyll a, POC, DOC SPM concentrations) products of interest needed to develop specific inversion approaches allowing to face the different issues related to the optical complexity of coastal ecosystems.

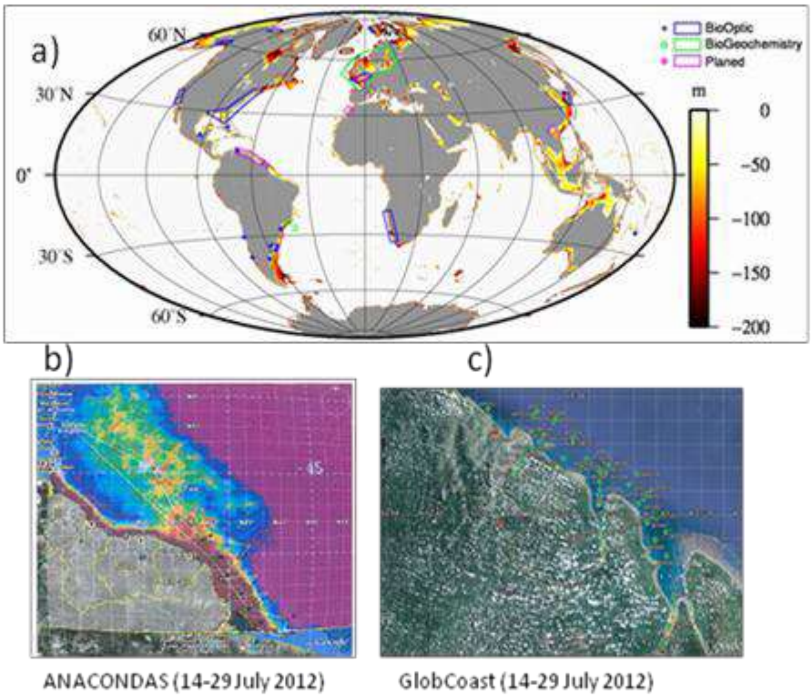

Figure 1: a) Location of the in situ data used in GlobCoast

These data are from various LOG, LEGOS, and GET cruises, the NASA/NOMAD data set, and other cruises performed in the frame of international collaborations involving some of the GLOBCOAST partners. b), c): Maps of the recent field campaigns already performed in the frame of GlobCoast and in collaboration with other research projects in French Guyana (GlobCoas), and from the Barbados to the Amazone River (ANACONDAS cruise, WHOI).

While existing inversion methods will be compared in the first steps of the project (e.g. Loisel and Stramski, 2000; Loisel et al., 2006; Lee et al., 2002; Maritorena et al., 2002; Morel and Gentili, 2009), the development of innovative approaches (Jamet et al., 2010, Vantrepotte et al., 2012) will also be considered in the context of GlobCoast. In particularly, the inversion of IOPs and biogeochemical products will performed using an approach based on the optical classification of the coastal domain. In practice, prior to the inversion of bio-optical parameters in such complex environments, each satellite pixel will be classified according of its optical characteristics (Figure 2). Then class-specific algorithms will be applied for improving the accuracy of the different inverted parameters. Considering such a classification approach within the inversion scheme should allow to reduce the dispersion usually found in the IOPs-Biogeochemical Components (BC) relationships, and then to significantly improve the retrieval of biogeochemical components.

For that purpose, mean specific IOPs values and reflectance spectral shape for each class should be established. This will be performed from an optical and biogeochemical data base gathering existing measurements which will be supplemented through dedicated cruised planned in the frame of GlobCoast including some cruises in the French Guiana Coastal waters (Figure 1). This would also help to better as to validate the products developed in the characterize this coastal domain at both an optical biogeochemical point of view as well frame on this ANR project.

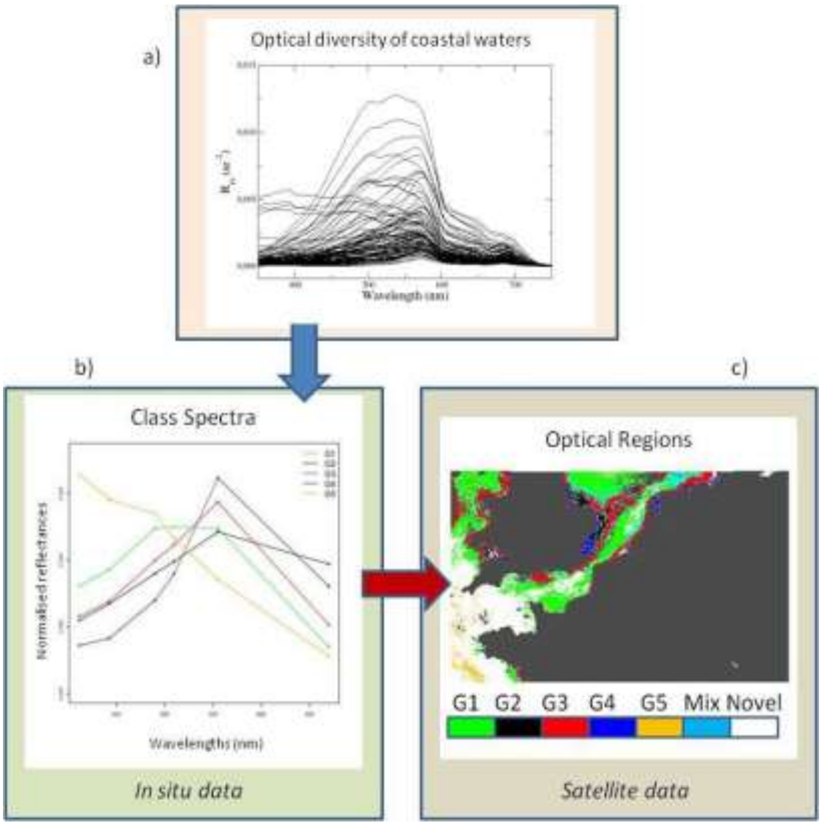

Figure 2: Methodology for the identification of optical water classes developed in the frame of GobCoast. The class-specific mean reflectance spectra (b) are obtained from classification techniques applied to a large data set of in situ reflectance (R_{rs}) spectra (a). Using novelty detection techniques, these classes will be compared to the satellite reflectance spectra to identify some homogeneous areas in terms of bio-optical properties (c)

Note that different approaches will be also used in the frame of GlobCoast for developing innovative atmospheric correction schemes in order to improve the accuracy of the normalized water-leaving radiance (nL_W) retrieval which often limit our ability to derive valuable satellite signal in coastal waters (Jamet et al., 2011). This will be for instance specifically performed through an optimization technique like the POLYMER algorithm (Steinmetz et al., 2011), developed by Hygeos.

2.2 Analysis of the inter-annual and decadal variability of the coastal ecosystems

Major patterns of temporal variability for the bio-optical and biogeochemical parameters (Task 3) as well as for sea surface temperature, wind and SSH will be described over the global coastal waters. The different ocean color products aimed in the context of the GloabCoast project will be assessed for the SeaWiFS (1997-2011, MODIS (2002-) and MERIS (2002-2012).

Temporal changes in many physical variables (e.g. river outflow, upwelling indices, tides, etc) will also be described for the various coastal test sites, the dynamics of which are supposed to be highly heterogeneous. In practice, patterns of temporal variability for the various parameters collected will be characterized considering successive time scales:

1) First, the characteristics of the seasonal cycle relevant to the general dynamics of the various coastal ecosystems will be described through the assessment of basic statistics from annual climatology (minimum, maximum, peak duration….).

2) Second, time series, when sufficiently long, will be analyzed to define the major characteristics of inter-annual temporal variability associated with the environmental and biogeochemical data in the various coastal sites.

3) Finally, variations occurring at longer time

scales (i.e. decadal) will also be characterized for the selected coastal areas. The potential of comparing the chlorophyll loads provided by the Coastal Zone Color Scanner (CZCS) archive (1979-1986) to those derived from SeaWiFS (1997-2007) for characterizing changes in marine biogeochemistry over the last 2 decades will be investigated. Note that the availability of CZCS data is however too restricted for allowing p decadal analysis over the French Guiana coastal waters.

The different temporal patterns of biogeochemical parameters as well as their interactions with the various environmental forcing will be compared specifically over the Amazon- influenced coast (mainly French Guiana).

To achieve the previous objectives, advanced time series analysis techniques will be applied to the time series generated for the different ocean color optical sensors. For instance time series for the different ocean color record considered will be decomposed into terms representing a seasonal cycle, a trend and irregular variation using the Empirical Mode Decomposition methods (Huang et al., 1998) as well as the Census X-11 iterative bandpass filter algorithm (Pezzuli et al. 2005) which advantages for describing ocean colour seasonality (i.e. relative importance and year-to year stability) and non-linear long term patterns have been demonstrated (Vantrepotte and Mélin, 2011).

3. RESULTS AND DISCUSSION

The following sections present some of the preliminary results obtained over the French Guiana coastal waters in the frame of GlobCoast which provide some illustrations of the applications that will be performed in the frame of this project in the latter coastal region.

3.1. Application of the classification-based approach over French Guiana coastal waters

Based on a cluster analysis applied to a wide range of coastal waters, a recent study has demonstrated that class-specific mean R_{rs} spectra significantly differ from one coastal environment to another in relation to variation in the bio-optical properties (Lubac and Loisel, 2007). This approach has been recently developed in the frame of GlobCoast (Vantrepotte et al., 2012) emphasizing the interest of performing an optical classification of coastal waters for dynamically describing changes in the optical properties and therefore in the water masses quality of the coastal waters of French Guiana (Figure 3). The four optical water types which been identified until now allow to account for about 2/3 of the optical variability of these coastal waters. Further, the advantages of the classification-based approach for improving the accuracy in the SPM concentration from satellite remote sensing techniques have also been demonstrated.

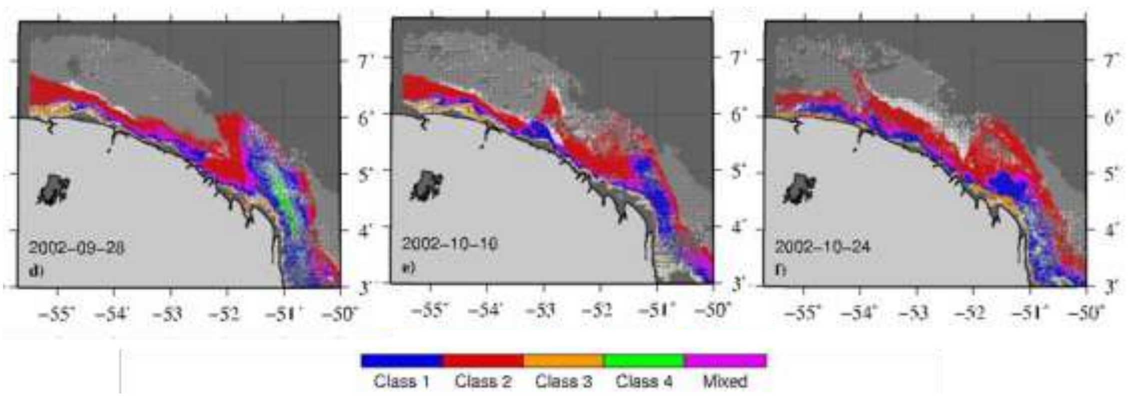

Figure 3: Daily illustration of the classification approach (from Vantrepotte et al., 2012) that will be developed and adopted in the frame of GlobCoast to assess bio-optical products from ocean color observations. Each color corresponds to a given bio-optical environment, for which specific bio-optical algorithm will be applied (Lubac and Loisel, 2007, Vantrepotte et al., 2012). This approach will allow the water masses optical quality to be dynamically monitored, and the retrieval accuracy of the marine products to be improved.

3.2. Characterization of French Guiana coastal waters dynamics as revealed from ocean color remote sensing data.

First results computed from the application of the Census X-11 decomposition method on the SPM times series derived for the MODIS archive has allowed to emphasize the impact of the north Brazilian retroflecting current system on the coastal water of French Guiana which lead to strong irregular temporal variations in the particulate matter content over this coastal region. Furthermore, the analysis of long term trends in SPM in the Guianese coastal waters has revealed the presence of peculiar alternating increasing and decreasing patterns which have been related to the impact of mud-bank migration over this coastal region (Figure 4). Further, specific results obtained over the French Guiana coast have illustrated the potential of ocean color data for precisely monitoring the dynamics (e.g. assessment of migrations rates) of mud banks over long time scales which will potentially allow for a discrimination of the environmental forcings driving these complex geomorphological processes (Vantrepotte et al., under review).

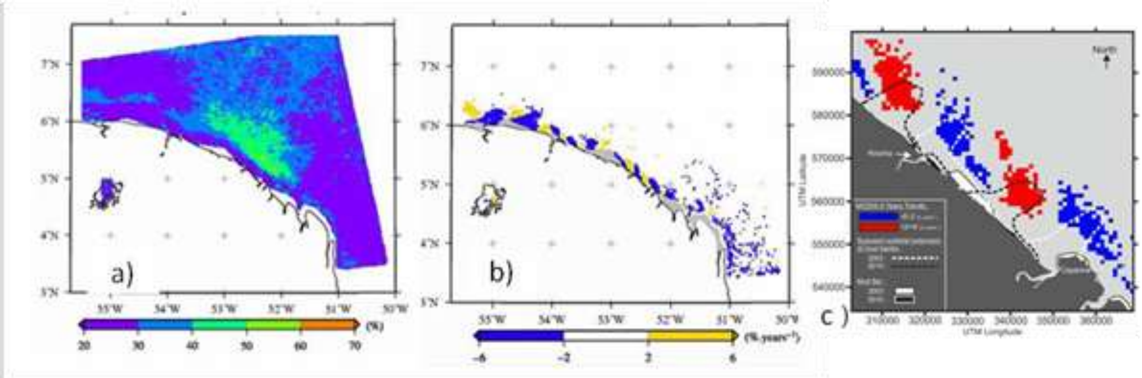

Figure 4: Application of the Census X-11 (Vantrepotte and Mélin, 2011) method for analyzing the temporal variation patterns of suspended particulate matter, SPM, in the French Guiana coastal waters over the MODIS period (2002-2010). The temporal variability in a large area offshore French Guiana is mainly explained by irregular variations (a) presumably associated with the formation of hydrodynamic rings linked to the north Brazilian retroflection current system. Significant trends in the SPM contents over this 8-yr period b) (Guianese coast) and c) (French Guiana) shows a clear alternation between increasing and decreasing areas that might be associated with the migration of mud banks particularly dynamic in this coastal region (Vantrepotte et al., under review).

4. CONCLUSION

French Guiana coastal waters (and more largely coastal waters influenced by the Amazon river outputs) will be specifically investigated in the frame of the ANR GlobCoast project. The different optical (IOPs, Kd) and biogeochemical (Chla, POC, DOC, SPM) descriptors which will be assessed from innovative approaches in the frame of this project will provide new and crucial information for understanding the biogeochemical processes occurring in the latter coastal domain. In particularly, the analysis of the time series generated for the various optical sensors considered in the frame of this project (SeaWiFS, MODIS, MERIS) will provide relevant insights on the dynamics of French Guiana coastal waters. The various scientific

achievements planned in the context of the GlobCoast project will in particularly help to better characterize the impact of the Amazon river outputs and related hydrodynamic processes on the biogeochemical dynamics of the Guianese ecosystems. As a matter of fact, some of the GlobCoast outputs will for instance provide precise information helping to better characterize and understand the dynamics of complex geomorphological processes (i.e. mud banks migration) occurring over the Guianese coast.

REFERENCES

Huang, N. E., Shen, Z., Long, S. R., Wu, M. C., Shih, H. H., Zheng, Q., Yen, N. C., Tung, C.C., Liu, H. H. The Empirical Mode Decomposition and the Hilbert Spectrum for Nonlinear and Nonstationary Time Series Analysis. Proceedings of the Royal Society of London A454 (1971): 903–995. doi: 10.1098 /rspa. 1998.0193, 1998.

IOCCG. Remote Sensing of Inherent Optical Properties: Fundamentals, Tests of Algorithms, and Applications. Lee, Z. (ed.), Reports of the International Ocean-Colour Coordinating Group, No. 5, IOCCG, Dartmouth, Canada. 2006, 89 p

IOCCG. Remote Sensing of Ocean Colour in Coastal, and Other Optically-Complex, Waters. Sathyendranath, S. (ed), Reports of the International Ocean-Colour Coordinating Group.2000, pp. 140.

Jamet, C., Loisel, H., Kuchinke, C.P., Ruddick, K., Zibordi, G., Feng, H. Comparison of three SeaWiFS atmospheric correction algorithms for turbid waters using AERONET-OC measurements. Remote Sensing of Environment 115, 1955–1965, doi:10.1016/j.rse.2011.03.018, 2011.

Jamet, C; Loisel, H. and Dessailly, D. Empirical nonlinear determination of the diffuse attenuation coefficient Kd (490) in coastal waters from ocean color images, Proceeding SPIE7858, 785806, doi:10.1117/12.869730, 2010.

Lee, Z. Carder, K.L. and Arnone, R.A. Deriving inherent optical properties from water color:a multiband quasi-analytical algorithm for optically deep waters. Applied Optics, 41, 5755-5772, 2002.

Loisel, H., Nicolas, J.-M, Sciandra, A., Stramski, D. and Poteau, A. Spectral dependency of optical backscattering by marine particles from satellite remote sensing of the global ocean, Journal of Geophysical Research, 111, C09024, doi:10.1029 /2005JC003367, 2006.

Loisel, H. and D. Stramski, D. Estimation of the inherent optical properties of natural waters from irradiance attenuation coefficient and reflectance in the presence of Raman scattering. Applied Optics, 39: 3001-3011, 2000.

Loisel, H. and D. Stramski, D. Estimation of the inherent optical properties of natural waters from irradiance attenuation coefficient and reflectance in the presence of Raman scattering. Applied Optics, 39: 3001-3011, 2000.

Lubac, B., and Loisel, H. Variability and classification of remote sensing reflectance spectra in the eastern English Channel and southern North Sea, Remote Sensing of Environment,110, 45–58, 2007.

Maritorena, S., Siegel, D.A .and Peterson, A.R. Optimization of a semi-analytical ocean color model for global-scale applications. Applied Optics, 41, 2705-2714, 2002.

Morel, A. and Gentili B. A simple band ratio technique to quantify the colored dissolved and detrital organic material from ocean color remotely sensed data. Remote Sensing of Environement, 113, 998-1011, doi:10.1016/j.rse.2009.01.008, 2009.

Steinmetz, F., Deschamps, P.-Y., and Ramon, D., Atmospheric correction in presence of sun glint: application to MERIS, Optic Express, 9(10):9783-800. doi: 10.1364 /OE. 19.009783, 2011.

Vantrepotte, V., H. Loisel, H., Dessailly, D., Mériaux, X. Optical classification of contrasted coastal waters. Remote Sensing of Environment, 123, 306–323, doi:10.1016/j.rse.2012.03.004, 2012.

Vantrepotte, V., Mélin, F. Inter-annual variations in the SeaWiFS global chlorophyll a concentration (1997-2007), Deep Sea Research I, 10.1016/j.dsr.2011.02.003, 2011. Vantrepotte, V., Gensac, E., Loisel, H., Gardel, A., Dessailly, D., & Mériaux, X. Satellite assessment of the coupling between in wáter suspended particulate matter and mud banks dynamics over the French Guiana coastal domain, Journal of South American Earth Sciences, under review.

ACKNOWLEDGEMENTS

This research has been founded by the GlobCoast project supported by the Agence Nationale

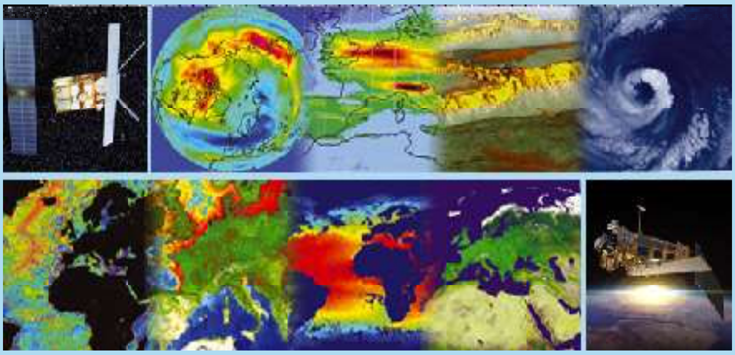

ESA promueve el desarrollo y la cooperación internacional

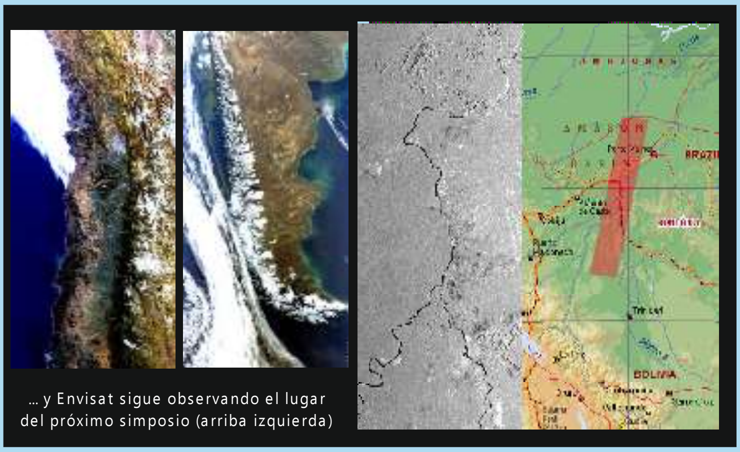

... y Envisat sigue observando el lugar
del próximo simposio (arriba izquierda)

ESA - ESRIN
Via Galileo Galilei,
Casella Postale 64.
00044 Frascati (Roma)
ITALIA
Tel: (39.06) 94180.409
Fax: (39.06) 94180.280
Att: Sr. Francesco Sarti (América Latina)

ESA - Asuntos Internacionales
8-10 rue Mario Nikis,
75738 PARIS Cedex 15, FRANCIA
Tel: (33.1) 5369.7731, Fax: (33.1) 5369.7627
Att: Sra. Marie Elisabeth De Vel (América Latina)

ECUADOR 1980 - 1983
CHILE 1983 - 1986
BRASIL 1986 - 1989
ARGENTINA 1989 - 1991
PERU 1991 - 1993
COLOMBIA 1993 - 1995
MEXICO 1995 - 1997
VENEZUELA 1997 - 1999
ARGENTINA 2000 - 2002
BOLIVIA 2002 - 2004
CHILE 2004 - 2006
COLOMBIA 2006 - 2008
CUBA 2008 - 2010
MEXICO 2010 - 2012
GUYANA FRANCESA 2012 - 2014